Validation of Atlantic salmon (*Salmo salar*) weight estimation by stereo camera, and morphometric analysis for assessment of growth performance and maturation status

Tina Emilie Lee Lange

This thesis is submitted in fulfilment of the requirements for the degree in Master of Science - Aquaculture

Department of Biological Sciences (BIO)

University of Bergen

April 2021

Acknowledgements:

First, I would like to thank my main supervisor, Jon Vidar Helvik, for helping me find this project and connecting me with my external supervisors. Thank you so much for all the effort you have put into this thesis, for always being available, and for helping me through this process. You have always been very positive, and had such a great enthusiasm and excitement for my work, which has inspired and encouraged me to stay positive and work hard throughout my entire thesis.

I would also like to thank my two external supervisors, Ole Folkedal and Jonatan Nilsson from the IMR, for putting in a huge amount of time into my master thesis, and helping me throughout the entire process. I appreciate you for always taking time to answer/respond to emails and video meetings, and for giving me constructive feedback, especially through the writing process. Thank you for all the knowledge, literature, and insights, which I have used to my advantage when writing my thesis. Lastly, you have both been very helpful with implementing the statistics into my thesis.

Thanks to Ragnhild Valen, Jean-Baptiste Muliloto and Alok Saxena from Aquabyte. To Ragnhild, for setting me up with Aquabyte, answering my questions, and providing me with material. A special thanks to JB, for sticking with me throughout the entire process, providing me with information, and helping me with anything I needed. To Alok, thank you for helping me with essential material.

I would also like to thank Andreas Størksen Stordal for helping me with the statistics. Your expertise was truly needed, as I had no experience with R or how to process huge amount of data.

I am truly grateful to all of you, for contributing to the quality of my thesis. Also, I would like to thank you, Ørjan, for the support, encouragement, coffees, love, and laughter through this special time in lockdown and during the writing process.

Contents

Abstract:

Stereo image analysis of free-swimming farmed Atlantic salmon is today used for purposes such as individual size estimation and sea lice counting. This technology may in the future be used to score welfare and life history traits. This thesis aims for answering: 1. whether current stereo camera image analysis of size estimation reflects the true size distribution of caged salmon, and 2. whether morphometrical relationships of individual salmon, measured in images, can provide novel insights to growth performance and detection of sexual maturation. The data was collected from an experimental cage production with individually PIT-tagged salmon (n=4500 and n=2786 at harvest) that were manually size recorded multiple times over the production cycle. Stereo images were taken within the sea cage during the last 6 months prior to harvest. Individual images taken at harvest were linked with PIT-ID to enable individual comparison of recorded morphometrics with growth history.

Stereo images allow for frequent and numerous measurements of free-swimming salmon, but the precision in estimating individual fish size and accuracy of size distribution within sea cages are largely undocumented. Weight estimations of free-swimming fish based on stereo image analysis are here compared with the true size distribution of the fish at the average weights 2.0, 4.0 and 5.5kg, including a comparison at an individual level by the stereo images taken at harvest. The results show that stereo image analysis gives a highly accurate weight estimation on an individual and populational level, but can to some degree be sensitive to fish size segregation in swimming depth.

Morphometrical relationships of the salmon body, and knowledge of how this reflects the growth performance and sexual maturation is largely underexplored. The morphometric analysis includes the ratios of body height central/anal, eye diameter and head size vs. standard length, and are here compared with the harvest size of the fish, individual growth, and sexual maturation status. Harvest weight was reflected in growth rate already from ~50g size, and the largest fish had the highest body height central ratio, and the smallest fish had the largest head ratio. Sexually mature fish showed a clear difference to immature salmon for body height anal and head size, which may be used for detecting early signs of maturation. In conclusion, this thesis proves current stereo image analysis of size estimation as useful, and validate novel salmon morphometrics as relevant parameters for automatization in stereo image analysis.

1. Introduction

1.1 The use of stereo camera in aquaculture

Fish farming is a substantial industry in Norway, being the world's largest producer of Atlantic salmon (Olaussen, 2018; FAO, 2020). In spite of an increasing global market and demand for Atlantic salmon, growth of the production is restricted due to problems of environmental impacts, including sea lice and escapees (Olaussen, 2018; Overton *et al.*, 2019). Moreover, the mortality rate in salmon production is relatively high (~15%) for animal production (Jensen *et al.*, 2020; Grefsrud *et al.*, 2021), and it has not been improved over the last years (Stien *et al.*, 2019). This, together with an increasing use of cleaner fish that also has an unacceptable high mortality rate, constitutes to animal welfare problems (Stien *et al.*, 2020; Grefsrud *et al.*, 2021). Several and different technological innovations and production strategies are aiming for lessening environmental impact and improving the fish welfare and survival (Grefsrud *et al.*, 2021). Based on experience and frameworks from livestock farming, the concept of Precision fish farming (PFF) is introduced to improve monitoring, control, and documentation of biological processes in fish farms, which will be achieved by emerging technologies and automated systems (Føre *et al.*, 2018). Knowledge based industry development and decision making within production cycles of fish are thus the solutions for improved animal health and welfare, while increasing the productivity (Føre *et al.*, 2018). This will reduce dependencies on manual labor and increase the environmental sustainability in commercial intensive aquaculture, versus the traditional experience-based regime (Føre *et al.*, 2018).

In salmon aquaculture, knowledge of growth, health status and parasite load are crucial for production planning and operational adjustments to increase welfare and production efficiency (Asche *et al.*, 2018; Olaussen, 2018). For production planning, knowledge of weight and number of fish is essential for not exceeding the maximum total biomass (MTB) that a fish farmer is permitted to have in production in Norway, but also highly important towards timing of harvest and sale of the fish (Aunsmo *et al.*, 2013; Hersoug, 2015). Aunsmo et al. (2013) investigated the industry precision and accuracy of the salmon biomass estimation upon harvest in Norway, and found that >50% of estimates fall out of 3% errors. For operational use, knowledge of the fish size distribution and growth pattern, including the condition factor of the fish, should indicate current status as well as the scope for growth within any fish group (Aunsmo *et al.*, 2013; Føre *et al.*, 2018). This should also provide important feedback for feeding control and detection of disease, stress, or deteriorating environmental conditions (Aunsmo *et al.*, 2013).

Poor fish health status makes the fish vulnerable for lice treatments, diseases, and salmon lice, and contributes to increased production costs (Assefa and Abunna, 2018; Overton *et al.*, 2019). The salmon industry has a huge challenge battling with salmon lice (*Lepeophtheirus salmonis),* where treatments requires handling, which often inflicts poor welfare and increased mortality rates of the fish (Oppedal *et al.*, 2011; Overton *et al.*, 2018). The salmon lice is an ectoparasite which reside in the uppermost parts of the seawater (0-10m) of the northern hemisphere, and prey only on salmonids (Heuch *et al.*, 2005). The infection rates on both wild and farmed salmonids has increased with the growth of the salmon industry (Costello, 2009; Aunsmo *et al.*, 2013; Thorstad *et al.*, 2015). To limit the problems, governmental biomass restrictions has been applied through the traffic light system to regulate further growth in vulnerable areas (Jansen *et al.*, 2012; Nærings- og fiskeridepartementet, 2020).

In the recent years, the innovation and use of different aquaculture technologies has modernized and developed the industry. New boats for transport, harvest, delousing and medical treatment has been developed, as well as new sea cage constructions (open, semi-closed, and closed) (Noble *et al.*, 2018). Other technology development lies in automation of fish monitoring, that is rapidly advancing by stereo and online cameras in sea cages (Føre *et al.*, 2018). Stereo image monitoring of free-swimming fish is carried out by the use of submerged cameras connected to image analysis (Costa *et al.*, 2006; Føre *et al.*, 2018). Ordinary sub surface cameras are commonly used in salmon farming, and predominately for online monitoring of fish appetite (behavior and pellets) and farm structures (Beddow *et al.*, 1996; Ang and Petrell, 1997). More advanced systems such as stereo cameras are less common, and can be used for measuring fish size (i.e. growth) (Hao *et al.*, 2016), automatic detection, and logging of sea lice (Tillett *et al.*, 1999) and other characteristics lined with fish welfare (Noble *et al.*, 2018). The data acquired from direct visual observation are qualitative and quantitative information based on the bio-responses of salmon (Føre *et al.*, 2018). The rapid expansion of computer vision technologies comes from enabling the hardware being developed in camera and computer technology, and the increased introduction to the consumer marked (Lecun *et al.*, 2015).

1.1.1 Information obtained from an image

There is a saying that comes from the editor Arthur Brisbane in 1911: "Use a picture. It is worth more than a thousand words" (Bouch, 2009). Since then, camera technology worldwide has developed rapidly, and so has the possibilities to deploy and extract information from images. Today we use camera technology combined with sophisticated software algorithms everywhere in our daily lives, for face recognition, surveillance, in medicine etc. (Tawalbeh *et al.*, 2016; Elish and Boyd, 2018). This has also been of interest for the salmon industry, and is the reason why several companies develop this technology for fish and underwater use (Beddow *et al.*, 1996; Føre *et al.*, 2018).

The information obtained from an image is limited to the image quality and by the use of human assessment or programed algorithms, and how well they extract information (Misimi *et al.*, 2006; Elish and Boyd, 2018). Applied to aquaculture, it is evident that underwater images can provide assessment of farmed fish such as salmon, which should enable similar valuation of the exterior of individual fish as commonly is done by inspection on land (Folkedal *et al.*, 2016). The morphometrics of fish can be read out from images, where size, deformities, sexual maturation, diseases, wounds etc. can be detected (Beddow *et al.*, 1996; Kadri *et al.*, 1997; Føre *et al.*, 2018). Images can be taken continuously, which gives security in large numbers, and the ability to follow individual or populational development throughout the production period.

1.1.2 Big data and AI

A great amount of computer power is needed to run processes involving Big Data and artificial intelligence (AI), aiming for processing and extracting useful information from a huge amount of data in a matter of seconds (Elish and Boyd, 2018; Olatunji *et al.*, 2020). AI is a technique which enables machines to mimic human behavior (Elish and Boyd, 2018). Developing the AI to be able to automatically count lice or estimate the weight based on images, is what some companies strive to achieve. To do this, the machine must be fed with a large amount of manually annotated images that are used to build up algorithms through machine- and deep learning (Lecun *et al.*, 2015; Olatunji *et al.*, 2020). Machine learning (ML) is a subset of AI, which uses statistical methods that enables machines to improve with experience, and deep learning is a subset of ML, which makes the computation of multi-layer neural network feasible (Lecun *et al.*, 2015). Biological evidence is, however, needed to facilitate, and to evaluate its output for further improvements (Elish and Boyd, 2018).

1.2 Possibilities with the use of camera technology in aquaculture

Several technological solutions have been designed for automatic estimation of individual fish size to assess growth at population level (Føre *et al.*, 2018). Optical measure frames (e.g. Storvik and VAKI) has been used in salmon farming for decades, and estimates individual body weight from shadow images (Beddow *et al.*, 1996; Haugholt *et al.*, 2010). Camera systems exploiting stereo photography for sizing of individual fish was launched as a product by AKVA in 2010 and relied on manual image processing (Haugholt *et al.*, 2010). Stereo photography relies on two cameras positioned from one another with a known distance, and the cameras takes one image each simultaneously, which combined makes is possible to measure depth and distances in an image (Costa *et al.*, 2006). Recent development in data processing and communication platforms have paved the way for automatic and increasingly advanced use of stereo image data (Føre *et al.*, 2018). Big data and AI is today used to process millions of pictures for pattern recognition of salmon and biomass estimation (Li *et al.*, 2020).

Combining existing underwater camera technology with automation of image processing, detection, and quantification of fish welfare indicators will save time and resources (Noble *et al.*, 2018). Over the recent years, automatic sea lice counting from underwater stereo images of free-swimming fish has been an aim for several companies and a driver of technological advancement. This relies on advanced algorithms for lice detection, and the images may be used for multiple purposes including identification of individual fish, size estimation, and welfare scoring (Stien *et al.*, 2017; Føre *et al.*, 2018; Noble *et al.*, 2018). Counting lice based on images in sea cages, which companies as e.g. Aquabyte and MSD does, relives fish farmers from manually counting lice every week, and provides continuous lice numbers based on a higher number of fish compared with traditional manual lice counts. Being able to use images to track the fish welfare, lice infestations levels and to estimate growth by development in size distribution in the pens every day, will be highly valuable for every fish farmer (Føre *et al.*, 2018; Noble *et al.*, 2018).

1.3 Using stereo images to weight estimate fish in sea cages

The traditional method to monitor biomass in a sea cage is by calculating growth based on feed use and mortality rates within a sea cage, and conduct periodic samples from the cage for controlling the estimates (Noble *et al.*, 2018; Li *et al.*, 2020). Manual size sampling by crowding and netting out fish can be very biased by the sampling method, and thus provide estimates that are not representative for the population (Nilsson and Folkedal, 2019). These estimates has also been found when attempting automatic size estimation, as fish size segregation with depth is common (Folkedal *et al.*, 2012; Nilsson *et al.*, 2013). Thus, the vertical position of the fish size estimation sensor, stereo cameras included, might very well affect the result (Beddow *et al.*, 1996). Main question to be asked when utilizing automatic sizing of fish with any tool is whether the size estimate of single fish is precise (i.e. shows the true size), and if the accuracy in measuring the size distribution is sufficient.

1.3.1 Morphometrical analysis of Atlantic salmon

Morphometrics is a quantitative analysis of the form (size and shape) to an animal, mostly between key points at the body (Handeland *et al.*, 1998), and morphometrical analysis have earlier been done on Atlantic salmon (Fig. 1.1) (Kadri *et al.*, 1997). Estimations of the fish size from lateral measurements have been done with and without the use of camera technology (Beddow and Ross, 1996). Accelerated growth in farmed salmon has shown to result in smaller eyes and brain, due to the body growing disproportionally faster, compared to wild salmon of the same age (Pankhurst and Montgomery, 1994; Devlin *et al.*, 2012). Differences in morphometrics between populations and different regions have been documented for salmonids, where the size of the head, body, and eye diameter were taken into account (Solem *et al.*, 2006; Solem and Berg, 2011). Individual based welfare indicators such as condition factor, wounds, bleedings, weight loss, eyes (damage, protruding or cataracts), deformities (body and jaws), gill-, snout-, and fin damage have been used to score and classify fish welfare (Noble *et al.*, 2018). Most of these fish exterior characteristics are overtly visible in a lateral fish image, and thus image analysis would be a great tool for detecting unwanted external developments in free-swimming fish (Føre *et al.*, 2018; Noble *et al.*, 2018). Using different kinds of morphometrics to see how salmon on an individual and populational level are developing, and if detecting e.g. sexual maturation or continuously being able to calculate the condition factor, or SGR through stereo image analysis, would be highly valuable for fish farmers.

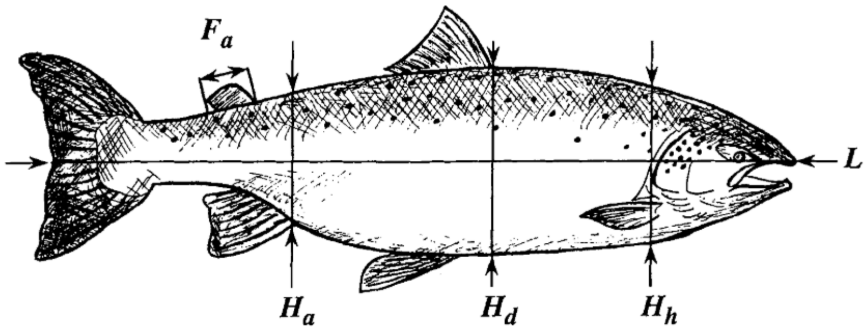

Figure 1.1: Morphometrical measurements of Atlantic salmon. F_a= adipose fin, H_a = body height prior to anal fin, H_d = body height prior to dorsal fin, H_h = head height and L: fork length. Image from Kadri *et al.* (1997).

1.3.2 The condition factor of fish

The condition factor, K, is calculated by using both weight and fork length (F1 in section 2.3.4), where the fork length is the length of the fish in cm (Fig. 1.1) (Stien *et al.*, 2013). The K-factor is divided into a system ranging from excellent (>1.6) to extremely poor (<0.9) (Stien *et al.*, 2013; Noble *et al.*, 2018). The values of K are usually between 0.9-1.6 and is often influenced by age, sex, season, stage of maturation, and fullness of gut, but also fat reserves and the degree of muscular development (Noble *et al.*, 2018). The condition factor of farmed Atlantic salmon increases with the size of the fish, and shows seasonal variations with water temperature, where the condition factor and growth tend to increase with warmer sea temperatures (Stien *et al.*, 2013; Noble *et al.*, 2018).

1.3.3 The specific growth rate of fish

The Specific Growth Rate (SGR) is calculated by using a known timeline and the change in weight (gained or lost weight) in that time frame for an individual fish or population (F2 in section 2.3.4) (Aunsmo *et al.*, 2014). The SGR indicates how many percent/day the fish has developed on average each day, where a positive number explains the amount of weight gain, and a negative number describes the amount of weight loss (Endal *et al.*, 2000; Aunsmo *et al.*, 2014; Noble *et al.*, 2018). The SGR for salmon is highly dependent on temperature, and decreases as the fish size increases (Skretting, 2012).

1.4 Detecting sexually mature salmon from image analysis

Sexually mature salmon show increased growth rate prior to showing overt morphometrical signs of maturation (Aksnes *et al.*, 1986; Taranger *et al.*, 2010), while maturation itself is an energy draining process, which gradually changes the physical appearance of the salmon (Fleming, 1998; Jonsson and Jonsson, 2009). Immature salmon, regardless of sex, shows an isometric weight-length relationship, while sexually mature salmon tended to grow allometrically (Leclercq *et al.*, 2010). Salmon with rapid growth have shown to have a positive correlation to early maturation (Taranger *et al.*, 2010). Size distribution for farmed salmon will vary in a population with the sex-ratio and maturation rate, which is due to dimorphism (Leclercq *et al.*, 2010). Oppedal et al. (2003) showed that the number and degree of maturating salmon varied, and that the maturating fish were mostly males. The timing of maturation in salmon, especially for males, varies and depends on external and internal factors, such as light, temperature, size, and lipid reserves (Simpson, 1992; Gutierrez *et al.*, 2014).

Images can be used to observe the development of sexually mature salmon (Beddow *et al.*, 1996). Kadri et al. (1997) looked at early separation of sexual maturating and immature salmon, where they investigated if it was possible to predict maturation based on the morphometrics, fork length, head height, and body height (Fig. 1.1). They concluded that there were no simple mathematical means for general discrimination between sexual mature and immature salmon, but the morphometrics could be used for visual grading (Kadri *et al.*, 1997). They studied the dorsoventral head axis to identify the difference between sexually mature and immature salmon, and not the anteroposterior head axis or jaw length. The anteroposterior head axis should be studied to conclude if there really is no difference in head size between sexual mature and immature salmon.

1.5 The diversity of growth in a population of salmon

In a population of farmed salmon, size is commonly normal distributed (Folkedal *et al.*, 2012; Nilsson *et al.*, 2013). Fish with a low condition factor, awful appearance, and arrested growth are often referred to as loser fish (Noble *et al.*, 2018; Fraser *et al.*, 2020). They fall behind, and in most cases dies from undernourishments or other causes (Stien *et al.*, 2013; Noble *et al.*, 2018). Fraser et al. (2020) showed how the environment or human application, like vaccination or handling, affected the number of loser fish in a population. Also, diseases (e.g. PD, CMS and PRV) can affect growth, mortality rates, and morphometrics of salmon (Aunsmo *et al.*, 2010; Løvoll *et al.*, 2010; Garseth *et al.*, 2018). There are several different strains and genetic differences within families of commercial salmon breeding programs, which shows different growth patterns up to smolt stage (Herbinger *et al.*, 1999) and during the sea phase (Thorland *et al.*, 2020). Thorland et al. (2020) studied dimorphism between sexes, where the body weight, fork length, and condition factor were studied. Males showed to have an 8% higher weight than females upon harvest, where the growth difference was shown to be established already at a mean population size of 0.5 kg (Thorland *et al.*, 2020). Size diversity arises from individual growth rates being affected by environmental impacts, treatments, parasites etc. (Fraser *et al.*, 2020). The use of multiple families is mostly done in research to gain understanding of genetics and scopes for selective breeding (Glover *et al.*, 2005; Macqueen *et al.*, 2008), while commercial aquaculture uses salmon with genetics that are proven as the most optimal combination of fast growth, low levels of sexual maturation, and good carcass quality (Quinton *et al.*, 2005; Thorland *et al.*, 2020). Selective breeding has been carried out for over 10 generations of salmon, where the objective is to achieve faster growth, higher feed utilization and reduced production time (Thorland *et al.*, 2020).

1.6 Objectives and aims

The objectives for this thesis are to validate Atlantic salmon weight estimation by stereo image analysis, and morphometric indicators for assessment of growth and sexual maturation status. Weight estimation from images of free-swimming salmon are compared with manually weighing of the fish, and images taken upon harvest is used to link individual fish growth history and maturation status with morphometrics of the body, eye, and head.

There are three main research questions that will be investigated:

Question 1: Does a stereo image analysis provide a precise estimate of weight? More specifically, how precise is the automated analysis in sizing of individual fish and how representative (accurate) are estimates of the fish size distribution?

Question 2: Does morphometrical relationship upon harvest represent differences in growth performances? More specifically, the morphometrical relationship (body height central, body height anal, eye diameter, snout-pectoral fin, snout-operculum, and upper jaw) vs. body weight, standard length and condition factor are tested for their correlation with fish body size and growth pattern.

Question 3: Can novel morphometrical relationship reflect if a salmon is sexually mature?
More specifically, can morphometrical relationship (body height central, body height anal, eye diameter, snout-pectoral fin, snout-operculum, and upper jaw) vs. body weight, standard length and condition factor be used to distinguish mature from immature salmon?

2. Material and method

2.1 Set up of the experiment

The experimental setup and fish production were determined from investigating the scope for breeding more stress tolerated salmon, which is not the scope of this thesis, but still provides a solid data set for individual fish growth. The experiment started in SalmoBreed where they selected 90 fish from 50 different families, in total 4500 fish. The selection of families was based on heritability estimation of harvest weight, where families with both low and high estimated harvest weight were chosen. Although, in this thesis the material was not based on the family differences, but looked at all the families as one population. The eggs of all families were hatched, and the fish was start fed within the same week to minimize the age gap, in SalmoBreeds breeding station at Lønningdal, Norway. The fish were tagged on the 18th of June 2018 with 12mm PIT-tags and measured for weight (15.94 ± 3.57g, mean ± SD). The salmon parr was then transported to the Institute of Marine Research, Matre Research Station in Matre, Norway, the 20th of June 2018, and evenly distributed over 30 tanks (500L), where each family was represented by three fish. All fish were sized three times during the freshwater phase in Matre, the 31st of July, the 29th of August during vaccination, and the 1st of October during smoltification. Half of the tanks were treated with elevated CO_2 levels (mg/L) from the 6th of August, until they were transferred into sea cages at the Institute of Marine Research, Austevoll Research Station in Austevoll, Norway, on the 5th of October 2018. The fish was evenly distributed into four cages (12 x 12m and 14m deep), consisting of half CO_2-treated and the other half not CO_2-treated fish. Two of the cages were repeatedly submerged with a regime of 6 days submergence to 1m depth followed by one day with surface access. The submergence treatment was carried out by attaching a net roof to the sea cage. The fish were manually sized during the seawater phase in January, June, September, December 2019, and at harvest in February 2020.

2.1.1 Treatments

The submergence regime was repeated, with one day of surface access per week, from the 26th of October 2018 until the 19th of June 2019, when a subsample of ~150 fish from each of the four cages (in total 568 fish) were taken out, measured, and welfare scored (SWIM, Stien et al., 2013). The SWIM test showed overt snout wounds on the submerged salmon, which resulted in the treatment being discarded to prevent further damage on the fish. The two submerged cages were gathered into one cage, and the two not submerged cages were gathered into one cage. This was to reduce the number of lice pr fish, as higher densities of fish has been shown to have lower lice infestation intensities (Samsing *et al.*, 2014). The fish were deloused five times during the seawater phase, and the first three was carried out by manually netting out the fish from the cage, where they were anesthetized and bathed for 30 seconds in a tank containing seawater of ~34°C (Folkedal *et al.*, 2021). The last two delousing events was carried out by a commercial treatment vessel (Thermolicer, Scale AQ). After the weighing in September 2019, all fish were gathered into one sea cage.

2.2 Camera set-up in the sea cage

2.2.1 Camera set-up in the sea cages

Stereo camera was put into the sea from September 2019 until harvest, to take stereo images of the fish during the seawater phase. The stereo camera used in the sea cage was one Aquabyte v2.1 stereo camera, which was a custom-made stereo camera designed internally by Aquabyte, coupled with machine- and deep learning. It was also equipped with LED-lamps on the sides (Fig. 2.1). The set up in the sea cage consisted of the camera and a circular PIT (Passive Integrated Transponder) antenna (50 cm Ø) fixated 1m in front of the camera. The fish had to swim through the PIT antenna to be registered. The camera and the PIT-antenna were mostly placed at 3m depth, but shifted between 2-10m on a few days to test different depths. There was only one antenna used during the majority of the experiment, but in January 2020 a second antenna was introduced to help link registrations to images (double PIT registration, i.e. before and after passing the camera).

Figure 2.1: Stereo camera used in the sea cages (Aquabyte), with LED-lamps on the sides.

2.2.2 Camera set-up and fish registration at harvest

At the harvest facility, all fish were bled out, before being photographed laterally on both sides by another custom-built stereo camera from Aquabyte (custom-built enclosure, Fig. 2.2A). The fish were also PIT-recorded, manually weighted, measured for standard body length, scored for SWIM indicators (Stien *et al.*, 2013), and opened for sex determination. The camera at harvest had a different enclosure, but the same optics as the one used in the sea. This was due to the in-air camera requiring less electronics, as it was coupled with external devices to run all the other processes, which the sea camera had to have built-in. The stereo images were automatically uploaded to a cloud server through the embedded system. All fish were individually registered by a PIT reader, and the PIT ID was then showed on a computer screen captured in the image, to be able to identify individual fish based on their PIT-tag (Fig. 2.2B). All images were loaded up to the server showing either the left or the right angle with a timestamp, where the unique PIT-tag IDs were manually linked to the image files.

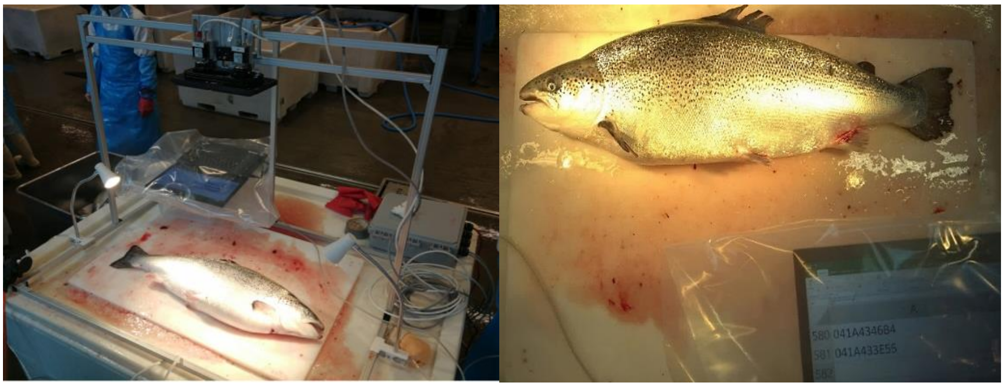

Figure 2.2: A: The camera setup at the slaughterhouse, displaying how the imaging of fish were done. B: Showing how the images uploaded to the server looked, with the corresponding PIT-tag in the lower left corner.

2.3 Manual sampling of the fish and sub selection for image analysis

2.3.1 Selecting a sub-group of 150 fish from the population

As mentioned above, all fish were manually weighed and measured for fork length seven different times (Table 2.1). From the harvest weight, 150 fish consisting of the 50 absolute smallest, 50 absolute largest and 50 individuals picked based on the average weight of the population. These three groups were carefully chosen to represent the extremes and mean of the population, and to be able to compare, measure, and detect differences within a population relative to weight, but also for discovering when the difference in fish sizes were established (starting at ~50g).

Out of the 50 families 45 was represented by the 150 fish, where 30 families where represented by 1-3 fish, 14 families by 4-7 fish and one family being overrepresented by 11 fish. The overrepresented family consisted of 9 fish from the large group, and one from both the medium and small group. The largest fish were represented by 23 families, the medium 29 families and the small 25 families, where 32 families were represented by at least two of the groups. In total, seven different groups were defined: the entire population, the selected 150 fish, 50 large, 50 medium, 50 small, 50 mature and 50 immature salmon. The sexually mature salmon were picked based on the December weighing, which confirmed the salmon to be mature, while the immature salmon were randomly picked based on the harvest data that confirmed them be immature. Both groups were chosen regardless of size.

Some of the non-stereo images obtained from harvest were not useable. In some images the fish was partly masked by the examinators hand or by ice slush, which obstructed the view of the fish within the image, and made it hard to measure the fish in ImageJ or use it for visual identification. The stereo cameras took one image pr second, and for a few fish, the fish were moved too fast so that only one side or no side at all was captured of the fish. Thus, the five groups consisting of small, medium, large, mature, and immature salmon had to be chosen from clear images showing the entire fish, that could be used to measure the different morphometrics of the salmon. Luckily there was only a few images that had to be removed, so that the 50 smallest and 50 largest fish represented the 50 smallest and 50 largest fish from the population. The medium, sexually mature, and immature fish were chosen based on good images of medium, sexually mature, and immature salmon. Another consideration of the imaging was the angle; if the fish were not laid directly underneath the stereo camera, measuring the height became difficult for those fish, as the angle could give the fish a different height.

2.3.2 Stereo camera and image analysis

Stereo image analysis was used to size estimate the fish in the sea, and to estimate different weight distributions based on sophisticated algorithms (Aquabyte). The salmon was PIT-registered, so that images from the sea were connected to the image of the same fish from harvest. This was to compare and see how the fish had changed from a particular day in the sea until harvest, and whether the algorithm, based on stereo image analysis, estimated weight that corresponded with the manually recorded weights of the same individuals. Skin pigmentation spot pattern recognition (Stien *et al.*, 2017) was used to confirm that it was the same fish.

The populational weight distribution estimates, based on stereo images, was done less than 10 days posterior to the September and December measurement, and less than 5 days prior to the harvest recording. Thus, the weight estimates had to subtract the weight the fish had gained during these days based on the SGR (%/day), to receive the same starting point as the manually weight recordings.

The fish were weighed after being bled out, each individual salmon was adjusted with an additional 2.82% of their body weight, representing the mean amount of blood lost (Nilsson & Folkedal, unpublished data based on 34 of the fish described in Thorland *et al.*, 2020, at harvest). When adjusted for blood loss, the resulting mean harvest weight was 5559.03 ± 1664.60g.

2.3.3 Measuring morphometrics in ImageJ

ImageJ (Wayne Rasband, NHI, USA) is a Java-based image processing program which allows the user to measure different lengths in an image (Schneider *et al.*, 2012; Schindelin *et al.*, 2015), and was used to measure the morphometrics (body height central, body height above the anal tract, eye diameter, snout-pectoral fin, snout-operculum, and upper jaw) of the salmon. The same format (pixel resolution) and distance from the fish to the stereo camera were used to compare lengths with the same scale between non-stereo images. The scale was calibrated by using a size reference or known distance, the metal frame (80cm), to be able to measure all lengths in the images in cm (Schneider *et al.*, 2012; Schindelin *et al.*, 2015).

The morphometrics of the salmon used in this thesis (Fig. 2.3) where standard length, body height central, body height anal, eye diameter, snout-pectoral fin, snout-operculum, and upper jaw. The standard length (red horizontal line), began from the snout and ended with the last tail bone, not including the fin. Kadri *et al.* (1997) used the fork length in their thesis which includes the tail, but I chose to use the standard length to prevent potential tail damages or the difficulties of finding where the tail ends, to affect the length measurement. Although, the manual measured length and the estimated length based on stereo images was measured for fork length, thus, the standard length is not compared to these two length measurements. The standard length measured in ImageJ for the selected 150 fish, and for the selected sexually mature and immature salmon, was used when compared to the morphometrical measurements, and not the fork length measured at harvest. Body height central (first red vertical line from the left), were measured vertically cranial of the dorsal fin. Body height anal (second red vertical line from the left), were measured vertically cranial of the adipose fin (above the anal tract). The eye diameter was measured horizontally (yellow line). There were three measurements for the head, the snout-pectoral fin (blue line), the snout-operculum (orange line), and the upper jaw (green line).

Usually the snout-operculum is the morphometrical measurement being used to measure the head length, but in commercial aquaculture the operculum has a tendency of being damaged (Rottmann *et al.*, 1992), causing the length of snout-operculum to be inaccurate. Also, finding where the operculum ends and how breathing affects the length measurement poses as a problem. Thus, the length from snout to the pectoral fin was also measured and used additionally, as the attachment of the pectoral fin could be found on every salmon. The upper jaw was measured to see if there was a difference between the head- and jaw size, between the three size groups, but especially between the sexually mature and immature salmon.

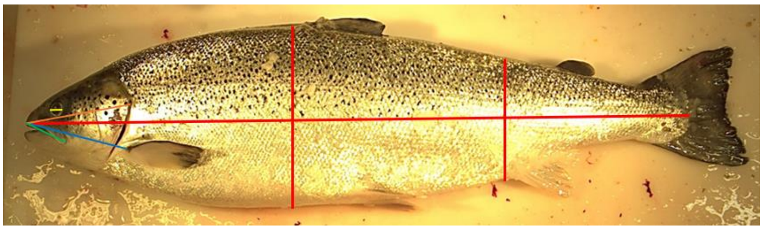

Figure 2.3: All seven morphometrical measurements done in ImageJ of the fish. Standard length without the tail (red vertical line), body height central (first red line from the left), body height anal (second red line from the left), eye diameter (yellow line), snout-pectoral fin (blue line), snout-operculum (orange line) and upper jaw (green line).

2.3.4 Condition factor and SGR formulas

The condition factor was measured by using formula 1: *K = 100*weight/fork length^3*. The specific growth rate (SGR) was measured by using formula 2: *SGR (%/day) = 100 * (LN (new weight) – LN (old weight)) / (new date-old date).* The date the fish were sized, the total number of measured fish, mean weight, mean fork length, condition factor, and SGR for the entire population is shown below (Table 2.1).

Table 2.1: The date the fish were sized, the total number of fish measured on the eight different dates and the mean weight, length, condition factor, and SGR for the entire population.

Date (dd.mm.yyyy)	N (total # of fish)	Weight (g ± SD)	Fork length (cm ± SD)	K-factor	SGR (%/day)
31.07.2018	4383	49 ± 8	15.0 ± 0.8	1.4	
29.08.2018	4433	71 ± 13	17.0 ± 1.0	1.4	1.2
01.10.2018	4437	93 ± 17	19.3 ± 1.1	1.2	0.8
22.01.2019	4261	463 ± 101	33.3 ± 2.3	1.2	1.4
04.09.2019	3490	2050 ± 584	54.7 ± 4.5	1.2	0.9
02.12.2019	3163	3980 ± 1272	64.2 ± 6.7	1.5	0.7
12.02.2020	2784	5559 ± 1665	70.0 ± 7.1	1.5	0.4

2.4 Disease

The Piscine Reovirus (PRV) was confirmed the 1st of April 2019, with moderate and high levels detected in fish from all cages. PRV is associated with heart and skeleton muscle inflammation (HSMI). The 19th of July 2019 the fish was sampled again for PRV, where the fish had low and moderate levels. Another test on the 26th of November showed moderate levels of PRV, as well as moderate and high levels of Piscine myocarditis virus (PMCV). PMCV is the causative agent for cardiomyopathy syndrome (CMS), and is a severe cardiac disease for farmed salmon (Løvoll *et al.*, 2010; Garseth *et al.*, 2018).

2.5 Statistical analysis

The data was analyzed by using R version 4.0.4 in RStudio to do all the statistical analysis and Microsoft Excel to make the figures and work sheet to use in R. The following packages were used in R (examples of R-scripts are found in Appendix A):

"RStudio (2021): Open source & professional software for data science teams. RStudio, PCB, Boston, MA. URL: https://rstudio.com/"

"J. Hester, H. Wickham (2020). Fs: Cross-Platform File System Operations Based on 'libuv', version 1.5.0. URL: https://CRAN.R-project.org/package=fs."

"H. Wickham, J. Bryan. Readxl, RStudio. URL: https://readxl.tidyverse.org."

2.5.1 Statistical analysis of stereo camera images compared to the manual size recordings

The estimated weight distributions of free-swimming fish, based on stereo camera image analysis for the September, December 2019 and February 2020, were compared with the manually measured weight distributions with an F-test to compare the variance and a Welch two sample t-test, were used to compare the mean weights.

When comparing the estimated size based on stereo camera images from harvest to the manual size recording for the entire population, a paired t-test was used. This was also done for the 150 selected fish.

2.5.3 Statistical analysis of the selected 150 fish and the comparison to the entire population

Comparing the weight and fork length for the 150 fish to the entire population was done by testing if the variance and means were different, this was done by using a F-test and a Welch two sample t-test. A Shapiro-test was used to test the normality of the distributions along with the density and q-q plot, where the population showed to be normally distributed in R (R-package “ggpubr”, ggdensity and ggqqplot were used). A one-way ANOVA was used on each of the seven manual weight recordings to test when during the fish production cycle a significant difference in weight or K-factor occurred between the three size groups. If there was a significant difference, then a Tukey HSD-test (R-package “multcomp”) was applied to see which of the three groups that differed from one another.

2.5.4 Statistical analysis of the morphometrical measurements for the 150 selected fish, and the mature and immature salmon

The morphometrics on the 150 selected fish, sexually mature and immature salmon were tested using a linear model (R-package “stats”) on each morphometrical measurement (body height central/anal, eye diameter, snout-pectoral fin, snout-operculum and upper jaw) compared to each of the explanatory variables (weight, standard length, and condition factor), to see if there was a covariance. For testing the correlation between all morphometrics and the weight, standard length, and condition factor, a Pearson’s product-moment correlation test was used. Then a one-way ANOVA-test was used on the morphometrical measurements for the 150 selected fish, to determine whether there were any statistically differences between the three size groups, and a Turkey HSD-test were applied afterwards. Comparing the head sizes with each other was done by using a paired t-test, for the head size measurements for the 150 selected fish. For the sexually mature and immature salmon, a Welch two sample t-test was used to test the difference in weight and standard length between the two groups. Testing the morphometrical difference between mature and immature salmon was done by using a Welch two sample t-test.

3. Results

3.1 Precision of individual size estimation based on stereo camera image analysis

Only four individual PIT-tag registered matches of free-swimming fish with the same individual photograph from harvest were confirmed (Fig. 3.1). The confirmed matches were from images taken within the last two weeks before the manual sizing in December (Table 3.1). The images illustrated how the fish had changed between November and harvest (74-81 days), where some lost (Fig. 3.1A-B) and others gained weight (Fig. 3.1C-H). The weight estimation of the sea images differed by 6.9, -15.8, 0.2 and -8.4% from the manual December weighing (mean dev.= -4.3%). The harvest images differed by 10.6, -6.9, -1.3 and 2.6% from the manual measured weights upon harvest (mean dev.= 1.2%, Table 3.1).

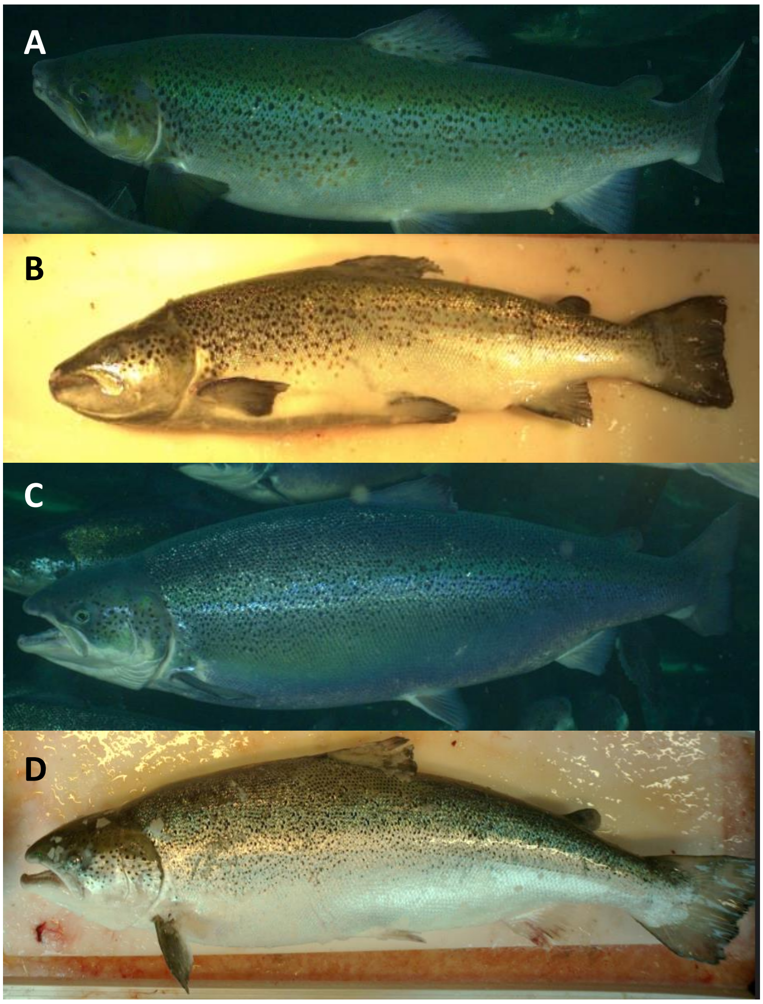

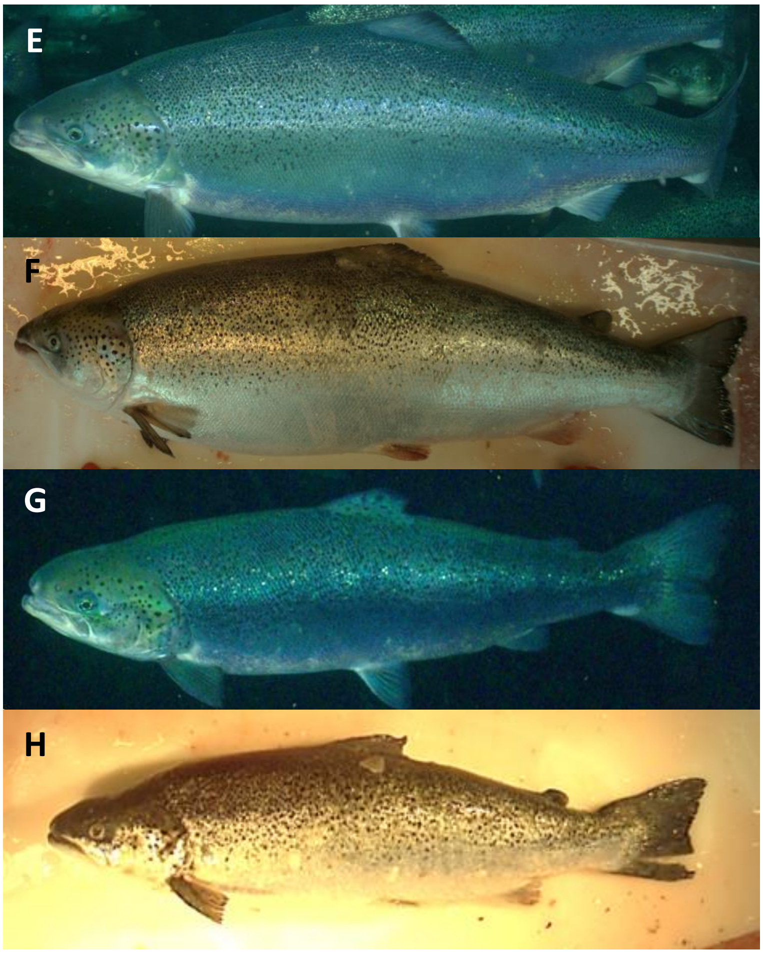

Figure 3.1: Fish 041A472ABF; A: in the sea, B: at harvest, 041A46C8F7; C: in the sea, D: at harvest, 041A47A6C0; E: in the sea, F: at harvest, 041A479EE8; G: in the sea, H: at harvest.

Table 3.1: The four individual fish which was identified based on PIT-code and their different measurements from September up until harvest. Weight, fork length, K-factor, and SGR are from the manual weighing and the weight estimation from the sea and harvest images were done by sophisticated algorithms.

Fish ID	**041A472ABF**	**041A46C8F7**	**041A47A6C0**	**041A479EE8**
Sept. weight (g)	1470	2430	3205	1260
Sept. fork length (cm)	52.0	63.0	63.0	48.5
Date of sea image (dd.mm.yyyy)	21.11.2019	26.11.2019	29.11.2019	27.11.2019
Weight estimation of sea image (g)	1979	6479	6369	1399
Dec. weight (g)	1842	7502	6355	1517
Dec. fork length	55.5	76.5	74.5	47.0
K-factor	1.1	1.7	1.5	1.5
SGR (%/day, Sept-Dec)	0.3	1.3	0.8	0.2
Weight estimation of harvest image (g)	1986	8253	8449	1761
Harvest weight (g)	1775	8765	8558	1715
Harvest fork length (cm)	55.0	81.0	82.0	46.0
K-factor	1.1	1.7	1.6	1.8
SGR (%/day, Dec-Feb)	-0.1	0.2	0.4	0.2

3.2 Stereo camera image analysis of the entire population and the selected 150 fish compared to the manual size recordings

3.2.1 Weight distribution based on stereo camera image analysis of free-swimming fish compared to the corresponding manual weight recordings

The estimated weight distribution compared to the manual weight distributions for the entire population on the sampling time points in September (2032 ± 652 vs. 2050 ± 584g, mean ± SD, deviation: -0.9%, p=0.11, Fig. 3.2A) and December 2019 (3963 ± 1122 vs. 3980 ± 1272g, deviation: -0.5%, p=0.46, Fig. 3.2B) showed no significant difference between the mean weights. The sophisticated algorithms overestimated the weight in February 2020 (5709 ± 1383 vs. 5559 ± 1665g, deviation: 2.6%, Fig. 3.2C), resulting in a significant difference in means (p<0.001) between the estimated weights and manually measured weights.

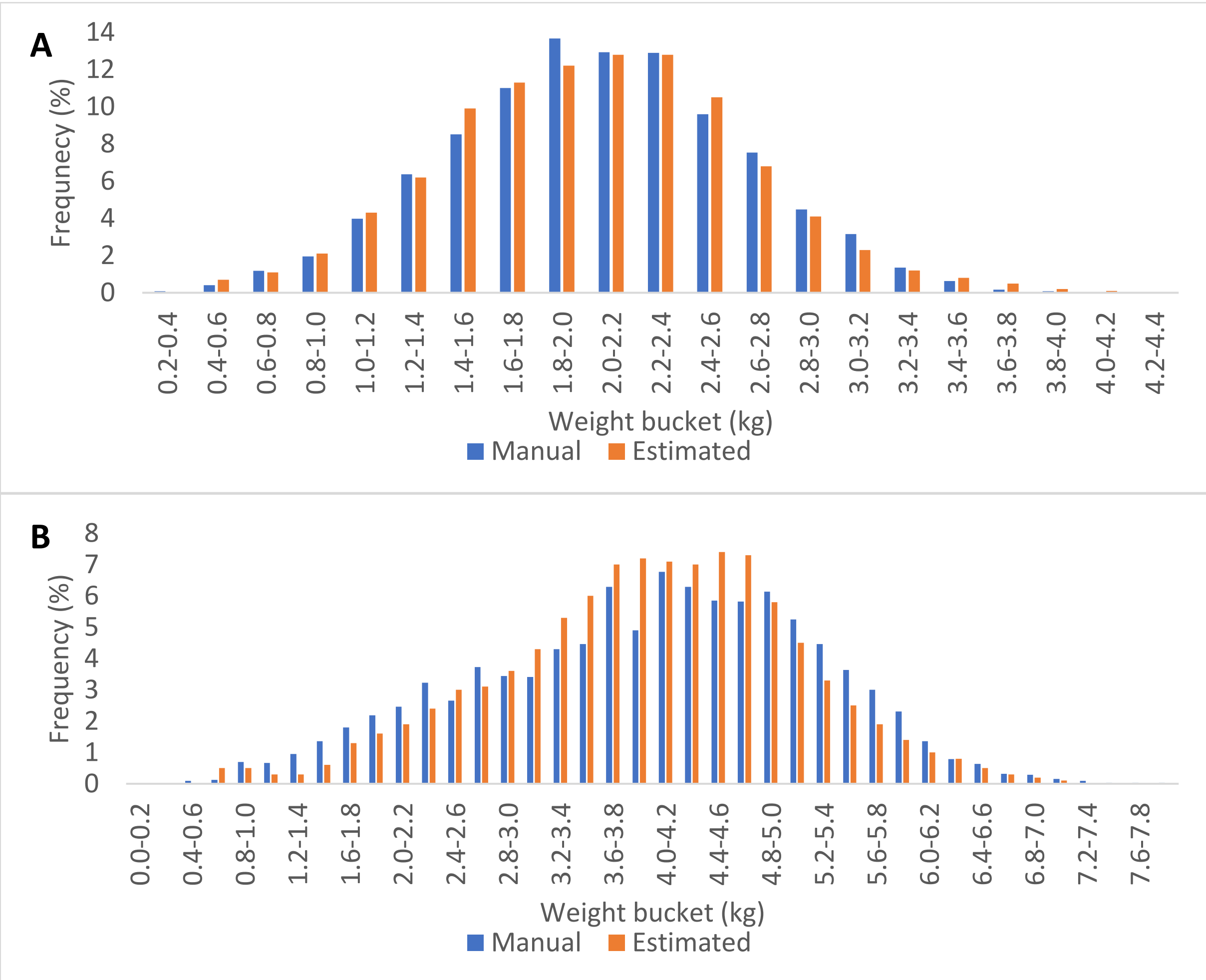

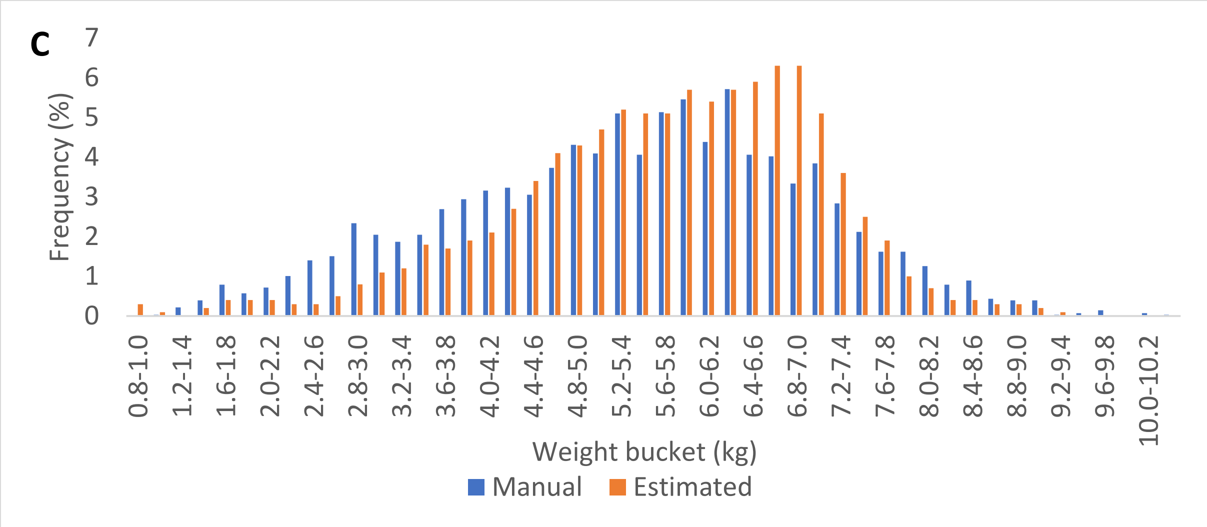

Figure 3.2: Comparison between the manual size recording and the estimated weight distribution in A: September 2019, B: December 2019, and C: February 2020.

3.2.2 Stereo camera images from harvest compared with the manual size recordings

3.2.2.1 Weight and fork length distribution of the entire population

The estimated weight based on stereo images taken of the entire population upon harvest, showed no difference in variance ($p=0.47$) when compared to the manual weight recording. A paired t-test showed that there was a significant difference between the individual weights ($p<0.001$, mean diff: 27g, Fig. 3.3A). The estimated fork length based on stereo images also showed to be significant when paired ($p<0.001$, mean diff: 2.0cm), compared to the manual measured fork lengths (Fig. 3.3B).

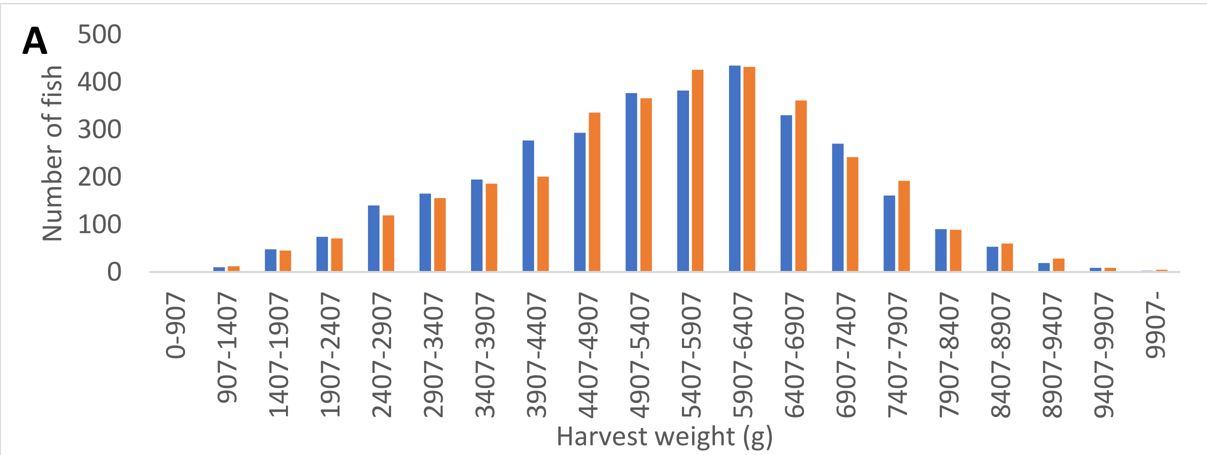

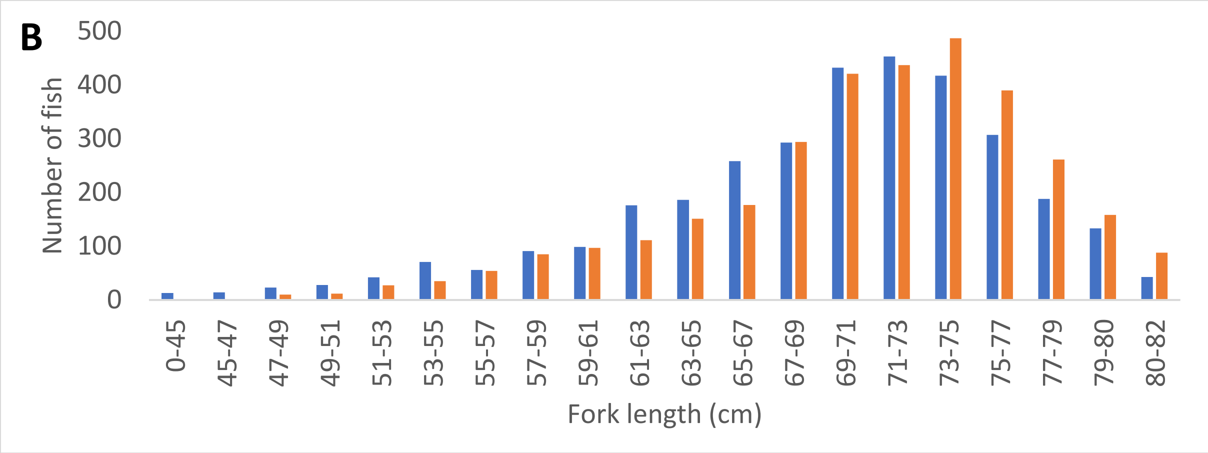

Figure 3.3: Comparison between the stereo camera image size estimation and the manual size recordings of the entire population based on the harvest images. A: manual weight recording (blue) compared with the estimated weight (orange), B: manual fork length recording (orange) compared with the estimated fork length (blue).

3.2.2.2 Weight and fork length distribution of the 150 selected fish

The estimated weights based on stereo images from harvest compared to the manual measured weights for the 150 fish, showed with a paired t-test no significant difference between the two groups ($p=0.34$, mean diff: 25g, Fig. 3.4A, Table 3.2). For the estimated fork lengths compared to the manual measured fork lengths, a significant difference was found when pairing the data for each individual fish ($p<0.001$, mean diff: 2.2cm, Fig. 3.4B, Table 3.2). The individual data for the 150 selected fish are shown in Appendix B (Table B.1).

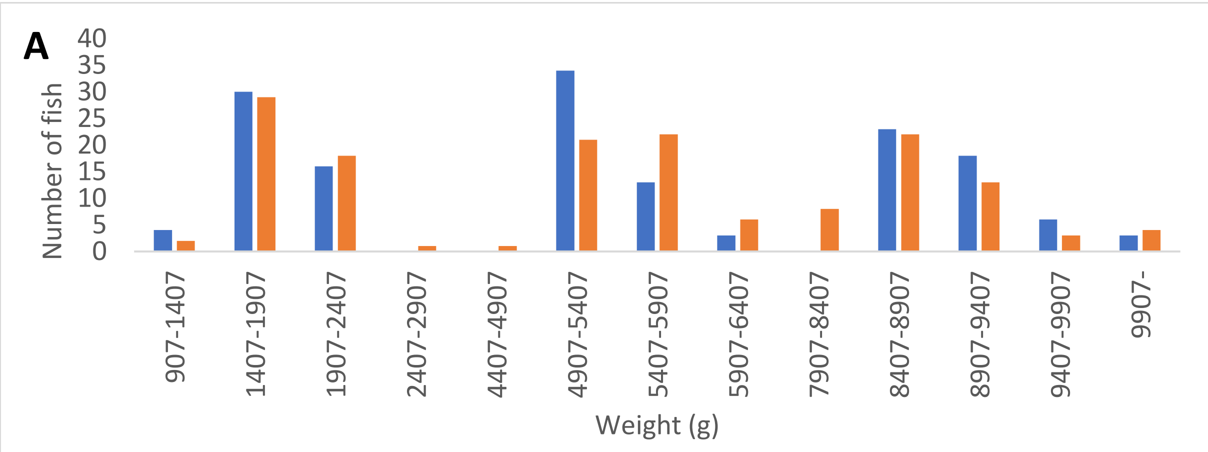

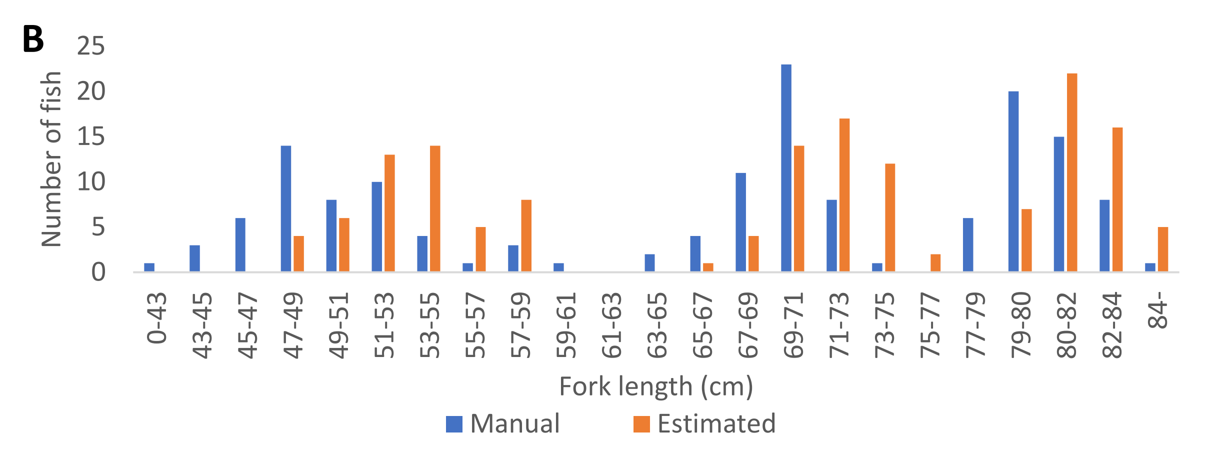

Figure 3.4: Comparison between stereo camera image analysis and manual size recordings for the 150 selected fish based on the harvest images. A: manual weight recording (blue) with the estimated weight (orange), B: manual fork length recording (orange) with the estimated fork length (blue).

Table 3.2: The mean weight and fork length for the 150 fish measured at harvest and the mean estimation of weight and fork length based on stereo images (Table B.1).

Fish ID	Weight (g ± SD)	Fork length (cm ± SD)	Estimation of weight (g)	Estimation of fork length (cm)
Large	8969 ± 462	81.6 ± 1.8	8855 ± 639	83.1 ± 2.1
Medium	5405 ± 232	70.6 ± 2.4	5388 ± 368	71.8 ± 2.1
Small	1713 ± 244	50.2 ± 3.5	1782 ± 317	53.4 ± 2.8

3.3 Analyzing the 150 selected fish and their morphometrics based on non-stereo images

3.3.1 Comparing the 150 selected fish to the population

The populational growth throughout the 7 size sampling timepoints showed to be more exponential for weight (Fig. 3.5A) than for the fork length (Fig. 3.5B). The harvest weight and fork length were substantially different for the large and small fish (Fig. 3.5A-B, Table 3.2), where the difference in fork length between the three groups did not occur until January 2019 ($p=0.02$). The 150 fish (49 ± 8g, mean ± SD, Fig. 3.6B) showed a significant weight difference ($p<0.001$) between the large (54 ± 7g), medium (50 ± 7g), and small (45 ± 8g) fish, already from the first weight recording. On an individual level, there was a huge difference in weight, where some of the individuals that were overlapping with the largest fish during the first four weighings (Fig 3.6B, D, F, H) ended up as the smallest fish at harvest (Fig. 3.6M). The correlation between the different weighings and the harvest weight varied from being negative, showing no correlation with the harvest weight during the first weighing for the small and large fish, to being positive during the last two weighings (Fig. 3.7). The medium fish had a positive correlation during the entire production, but the degree of correlation varied.

The population showed a decreasing condition factor until January 2019, where it stagnated towards September 2019, before increasing until harvest (Fig. 3.5C). The 150 selected fish showed a significant difference in condition factor from January 2019 ($p<0.001$), where the medium-large ($p=0.02$) and small-large fish ($p<0.001$) had a different condition factor, but no difference between the small-medium fish ($p=0.24$). For the last three dates, the small-medium ($p<0.001$) and small-large fish ($p<0.001$) showed to be substantial different, although the medium-large fish had a similar condition factor in both September ($p=0.37$) and December 2019 ($p=0.83$), before being significantly different upon harvest ($p=0.04$, Fig. 3.6M). The SGR, which was measured between each weighing, varied throughout the production but overall decreased with the increasing fish-size (Fig. 3.5D). The fish turned out to have the highest SGR between October 2018 and January 2019. Followed by an abrupt decrease in SGR until September. The tables with the mean values of weight (Table C.1), fork length (Table C.2), condition factor (Table C.3), and SGR (Table C.4) are found in Appendix C, as well as the growth development the selected 150 fish (Fig. C.1).

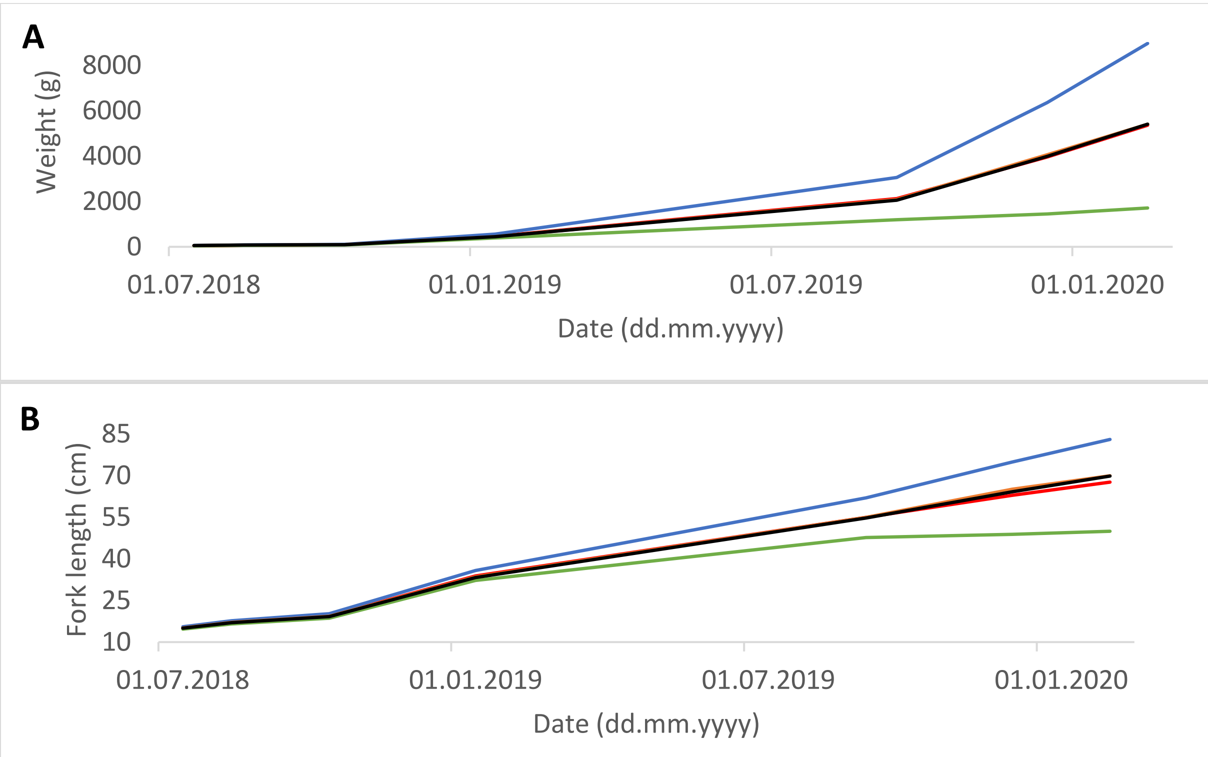

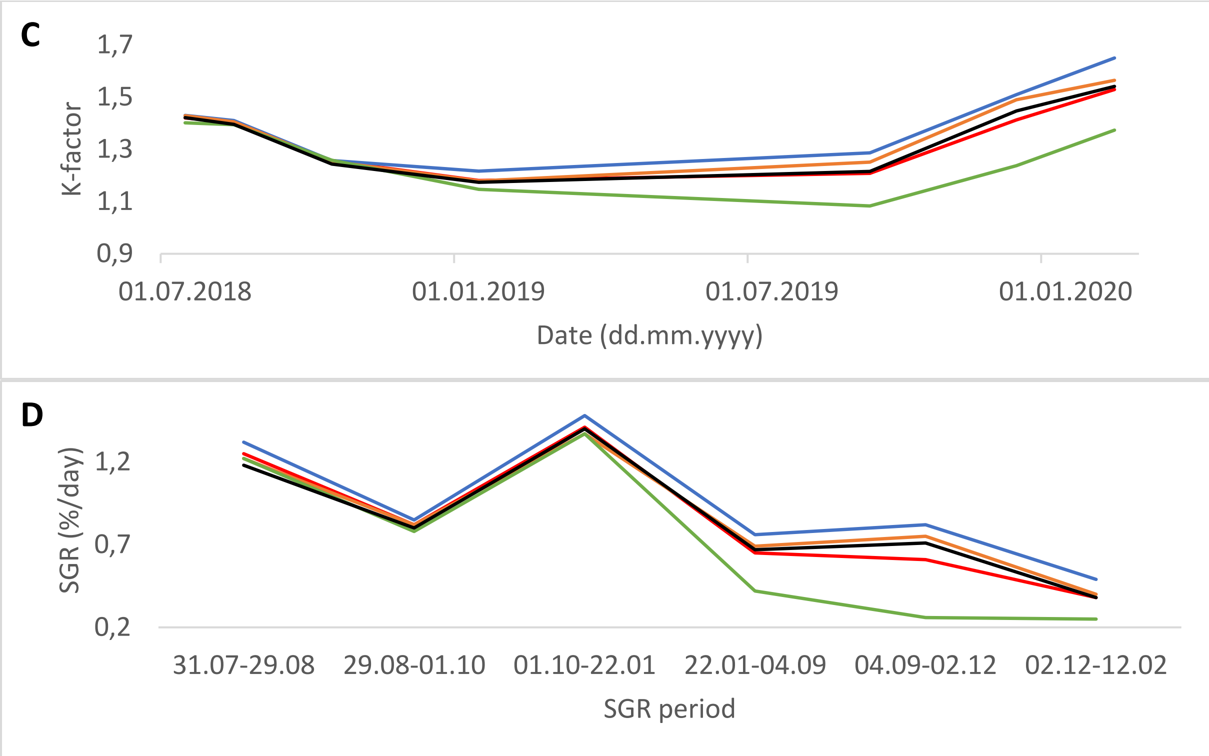

Figure 3.5: The average growth development for the entire population (black), the 150 fish (red), and the three groups consisting of small (green), medium (orange), and large (blue) fish during the production. A: weight, B: fork length, C: K-factor, and D: SGR.

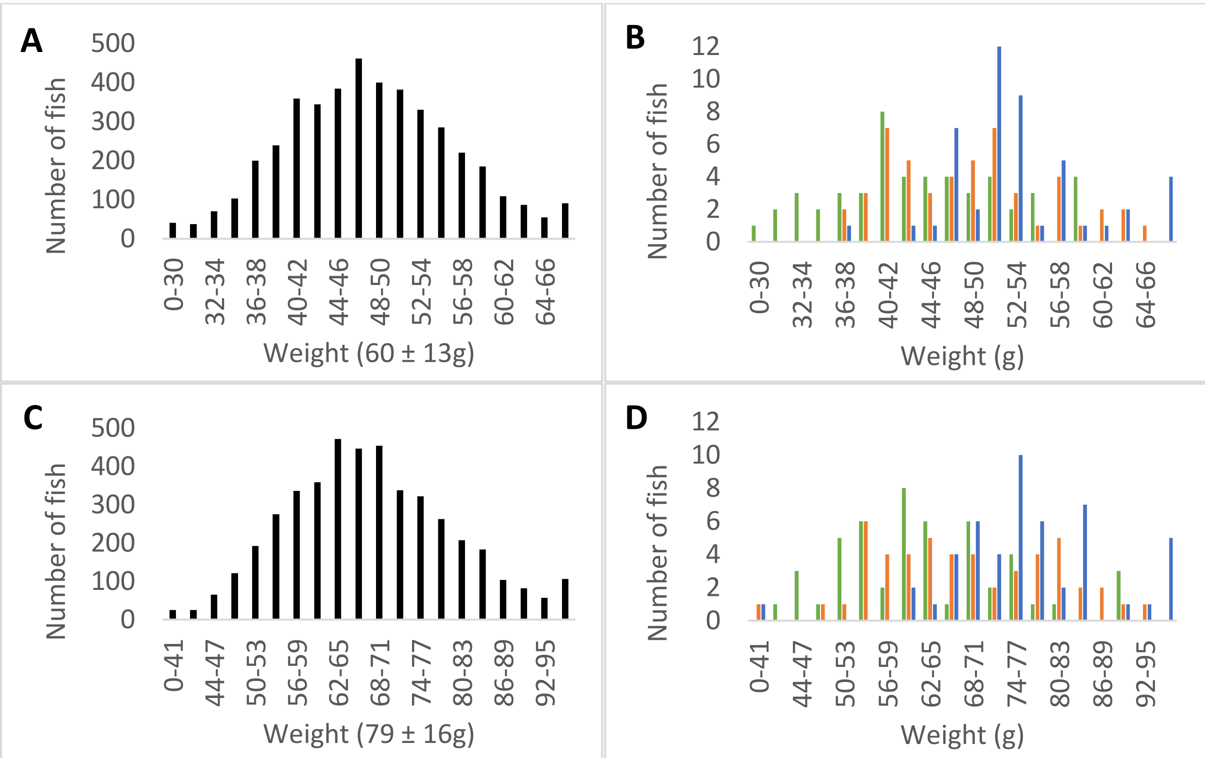

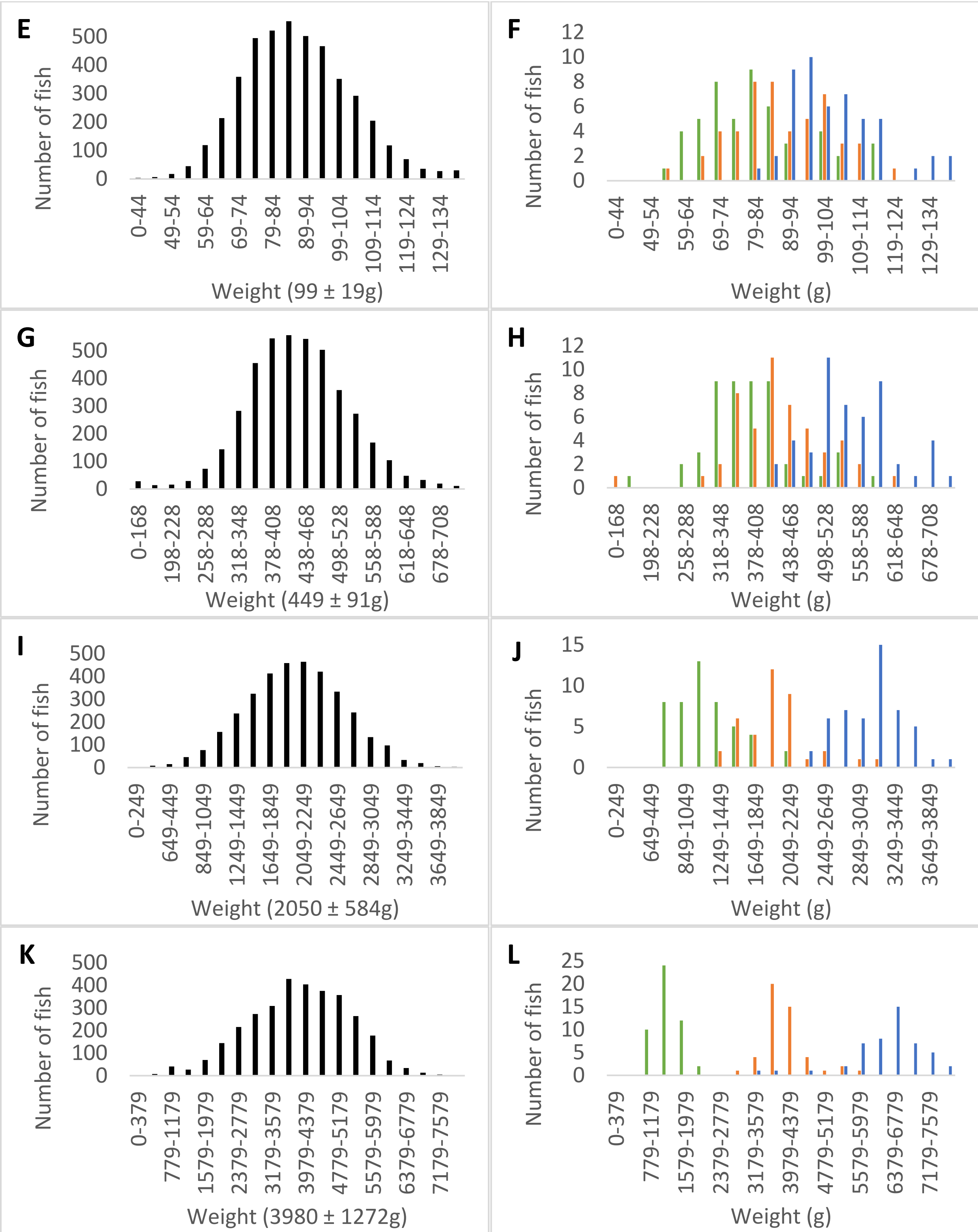
E
Number of fish
Weight (99 ± 19g)
F
Number of fish
Weight (g)
G
Number of fish
Weight (449 ± 91g)
H
Number of fish
Weight (g)
I
Number of fish
Weight (2050 ± 584g)
J
Number of fish
Weight (g)
K
Number of fish
Weight (3980 ± 1272g)
L
Number of fish
Weight (g)

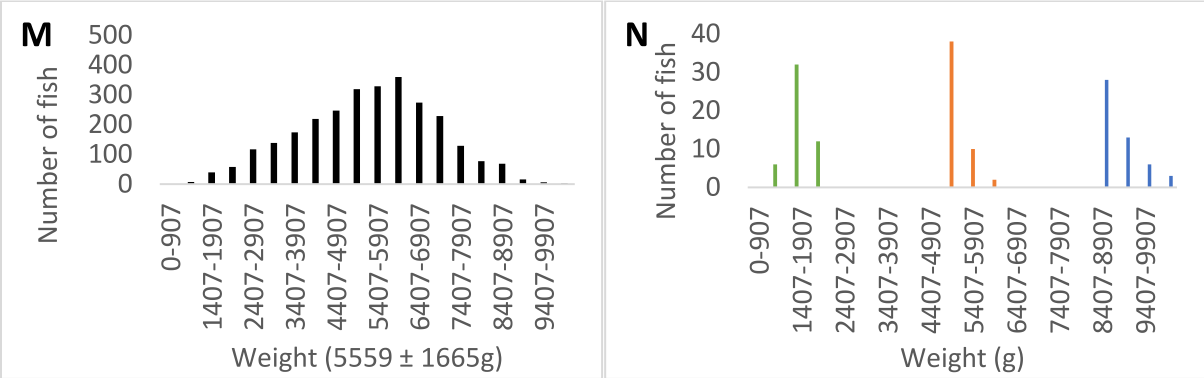

Figure 3.6: Weight distribution of the entire population (black) and the 150 selected fish, consisting of large (blue), medium (orange), and small (green) fish from the population, in July 2018 (A, B), August (C, D), October (E, F), January 2019 (G, H), September (I, J), December (K, L) and February 2020 (M, N).

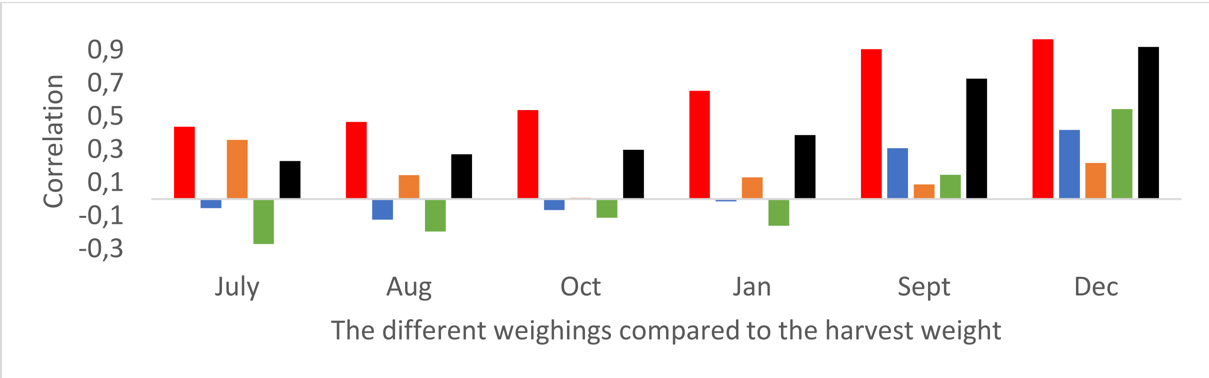

Figure 3.7: The correlation between the different weighings and the harvest weight for the 150 fish (red), the entire population (black), and the three groups consisting of small (green), medium (orange), and large (blue).

3.3.2 Comparison of large, medium, and small fish with non-stereo images

The group of large (Fig. 3.8A), medium (Fig. 3.8B), and small fish (Fig. 3.8C) had a corresponding mean condition factor of 1.7, 1.6, and 1.4 upon harvest. The mean specific growth rate for the last period (December 2019 - February 2020) was 0.5, 0.4, and 0.3 %/day respectively, which resulted in a weight gain difference (2606, 1287, and 260g) between the three groups. The largest fish consisted mainly of males (44/50 individuals), the medium of 17 males and 31 females, and the smallest fish consisted 25/25 of males and females. The missing tail length from the standard length done in ImageJ were on average 4.4, 3.8, and 3.3cm for the large, medium, and small respectively, which constituted to the standard length being on average 5.0, 5.2, and 6.1% shorter than the fork length.

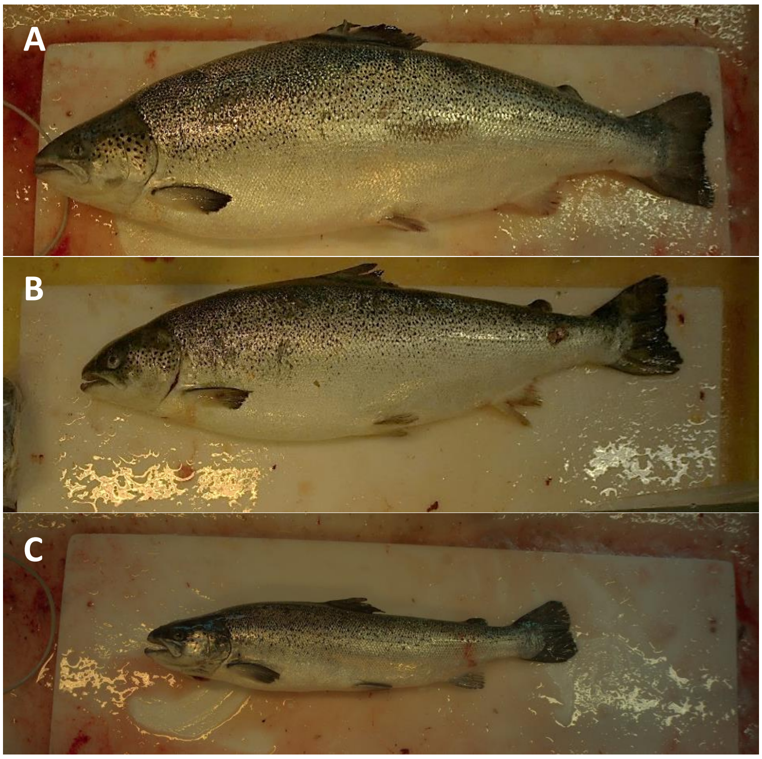

Figure 3.8: Image of the three size groups from the 150 selected fish upon harvest. A: a large fish (10190g, 84cm), B: a medium (5610g, 73cm) and C: a small fish (1680g, 54cm).

3.3.3 Analysis of the BHC and BHA for the 150 selected fish

Both the BHC and BHA ratio showed to have a significant correlation and positive correlation compared to weight ($p<0.001$, cor.=0.67, Fig. 3.9A and $p<0.001$, cor.=0.40, Fig. 3.9D), standard length ($p<0.001$, cor.=0.59, Fig. 3.9B and $p<0.001$, cor.=0.32, Fig. 3.9E) and condition factor ($p<0.001$, cor.=0.86, Fig. 3.9C and $p<0.001$, cor.=0.84, Fig. 3.9F), which signifies that the larger size of the fish, the higher the ratio. There was found a significant difference between the three size groups for the BHC ($p<0.001$, Fig. 3.9A-C), where the largest fish had the highest ratio compared to the medium and small fish (Table 3.3). The BHA ratio also showed a significant difference between the three size groups ($p<0.001$, Fig. 3.9D-F), but no difference between the medium and large fish ($p=0.23$, Table 3.3). The medium fish had a smaller difference between the two ratios (diff: 0.09, Table 3.3) compared to the large fish (diff: 0.11). The smallest fish had a significantly smaller ratio for both measurements ($p<0.001$, Fig. 3.9), and showed to have the smallest difference between the BHC and BHA (diff: 0.08) compared to the large and medium fish (Table 3.3).

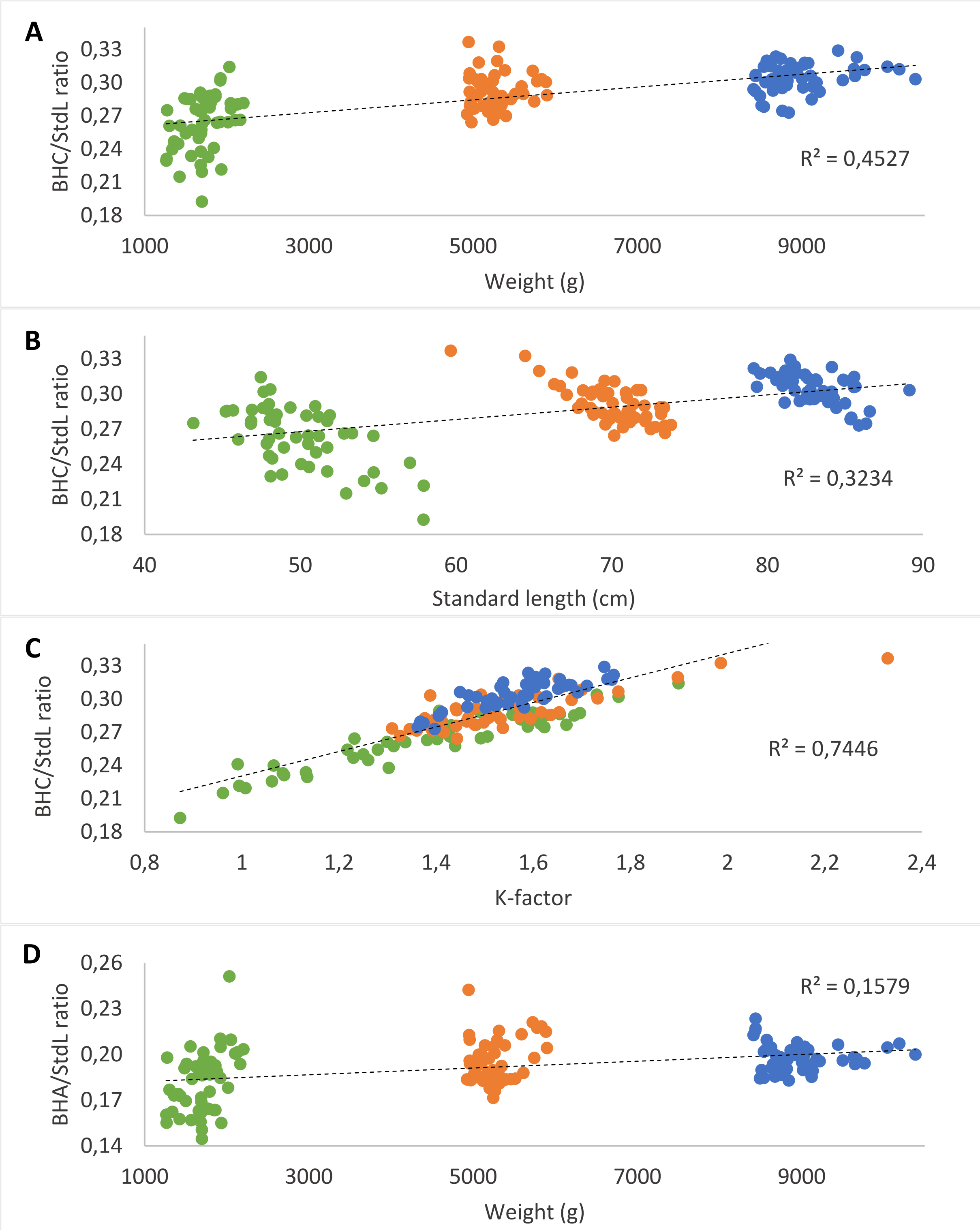
A
0,33
0,30
0,27
0,24
0,21
0,18
BHC/StdL ratio
1000
3000
5000
7000
9000
Weight (g)
R² = 0,4527
B
0,33
0,30
0,27
0,24
0,21
0,18
BHC/StdL ratio
40
50
60
70
80
90
Standard length (cm)
R² = 0,3234
C
0,33
0,30
0,27
0,24
0,21
0,18
BHC/StdL ratio
0,8
1
1,2
1,4
1,6
1,8
2
2,2
2,4
K-factor
R² = 0,7446
D
0,26
0,23
0,20
0,17
0,14
BHA/StdL ratio
1000
3000
5000
7000
9000
Weight (g)
R² = 0,1579

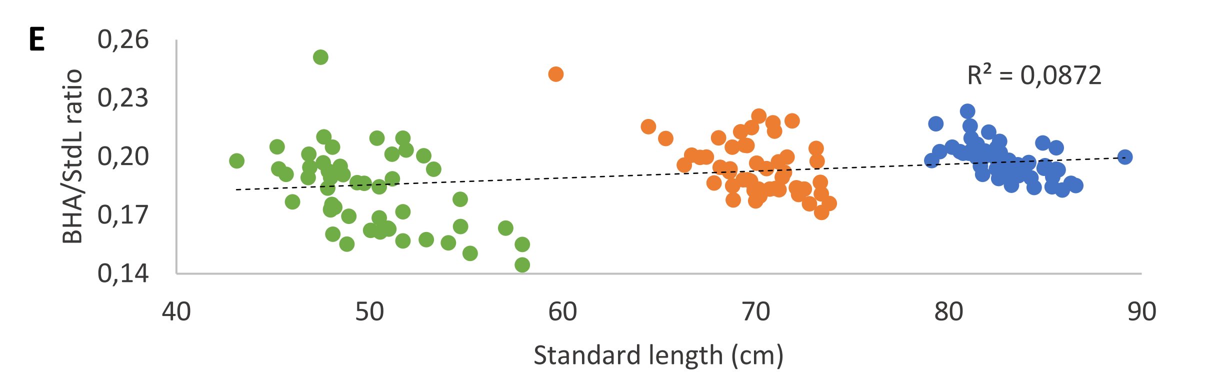

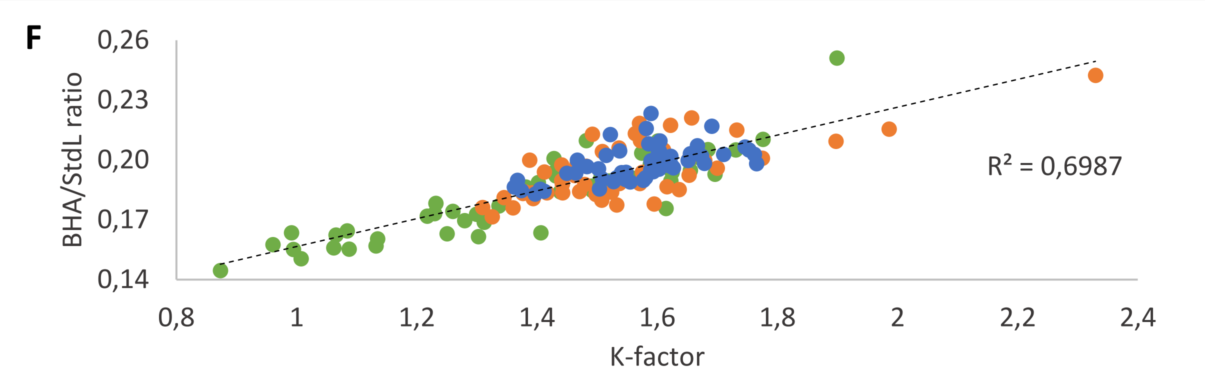

Figure 3.9: Morphometrics of the body height central (BHC) and body height anal (BHA) for the 150 selected salmon. BHC ratio compared to A: body weight, B: standard length, and C: K-factor. BHA ratio compared to D: body weight, E: standard length, and F: K-factor.

Table 3.3: The mean morphometrics for large, medium, and small fish, and the selected body measurements relative to standard length shown as ratio.

Morphometrics	Large fish (cm ± SD)	Ratio	Medium fish (cm ± SD)	Ratio	Small fish (cm ± SD)	Ratio
Standard length (StdL)	83.0 ± 2		69.9 ± 3		49.9 ± 3	
Body height central (BHC)	25.3 ± 0.9	0.31	20.3 ± 1.1	0.29	13.1 ± 1.0	0.26
Body height anal (BHA)	16.4 ± 0.6	0.20	13.6 ± 0.8	0.20	9.1 ± 0.9	0.18
Eye diameter	1.5 ± 0.2	0.02	1.4 ± 0.1	0.02	1.2 ± 0.2	0.02
Snout to pectoral fin	15.2 ± 1.4	0.18	12.7 ± 1.3	0.18	10.5 ± 1.1	0.21
Snout to operculum	15.1 ± 1.5	0.18	12.5 ± 1.3	0.18	10.7 ± 1.1	0.21
Upper jaw	7.0 ± 1.1	0.08	5.8 ± 1.1	0.08	5.0 ± 0.8	0.10

3.3.4 Analysis of the eye diameter

The eye diameter ratio for the 150 fish showed to have a significant negative correlation with the weight (p<0.001, cor.= -0.66, Fig. 3.10A), standard length (p<0.001, cor.= -0.66, Fig. 3.10B), and condition factor (p=0.03, cor.= -0.18, Fig. 3.10C). The eye diameter ratio was significantly different for the three size groups, where the largest fish had the largest eye diameter, but had the smallest eye diameter ratio compared to the medium and small fish (p<0.001, Table 3.3).

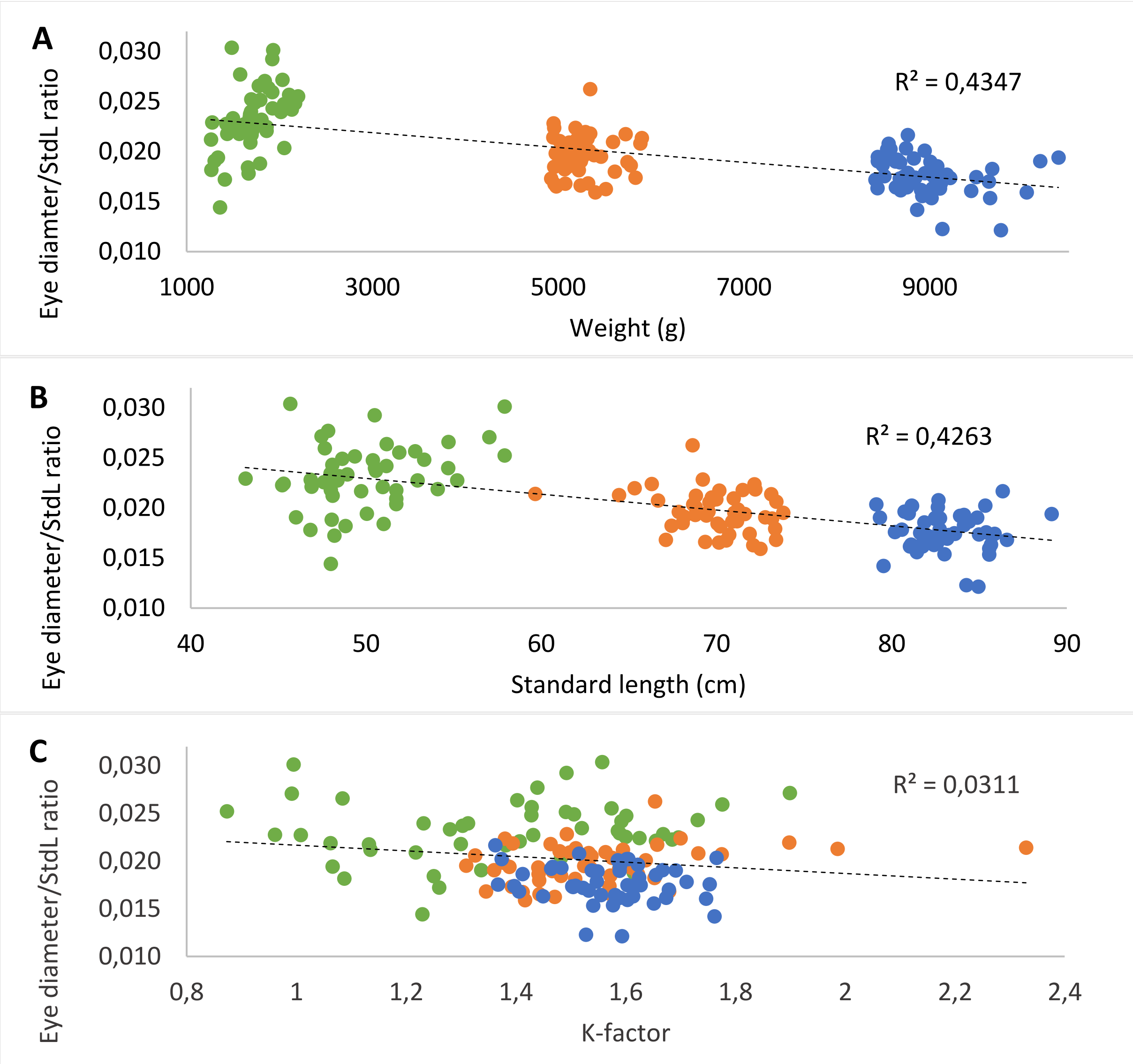

Figure 3.10: The eye diameter ratio for the 150 fish compared to A: body weight, B: standard length, and C: condition factor.

3.3.5 Analysis of the head size

All three head ratios (snout-pectoral fin, snout-operculum, and upper jaw), showed to have a significant negative correlation compared to the weight (p<0.001, cor.=-0.51, Fig. 3.11A), standard length (p<0.001, cor.=-0.53, Fig. 3.11B), and condition factor (p<0.001, cor.=-0.34, Fig. 3.11C). The length from snout-pectoral fin and the length from snout-operculum showed to be insignificantly different (p=0.95, paired t-test). The length of the upper jaw (5-7.0cm) and snout-pectoral fin (10-15.0cm) increased with the size of the fish, as well as the variance (5-8.0cm), resulting in a significant difference in length and variation between the snout-pectoral fin and upper jaw for all three groups of salmon (p<0.001). The pectoral fin ratio showed a difference in head lengths and that there was an effect of size groups (p<0.001), but no difference between the medium and large fish was found (p=0.94, Fig. 3.11). The figures of the snout-operculum length and upper jaw are presented in Appendix D (Fig. D.1).

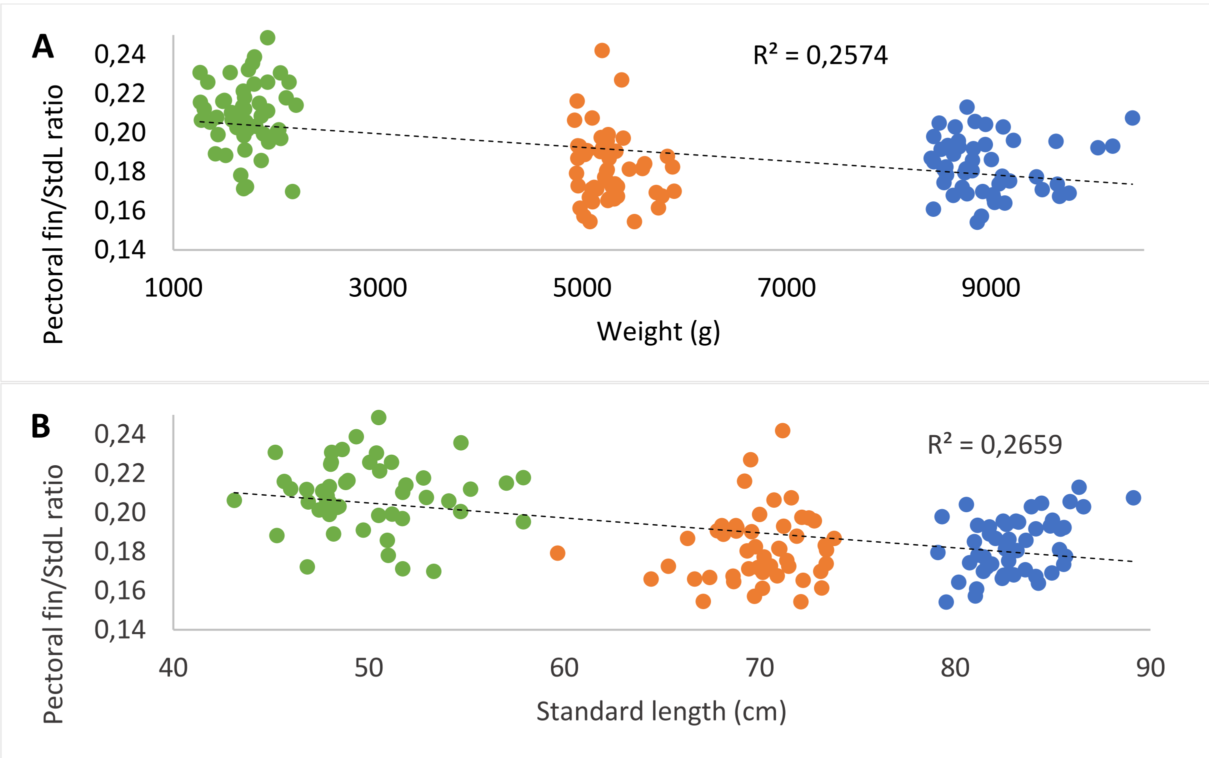

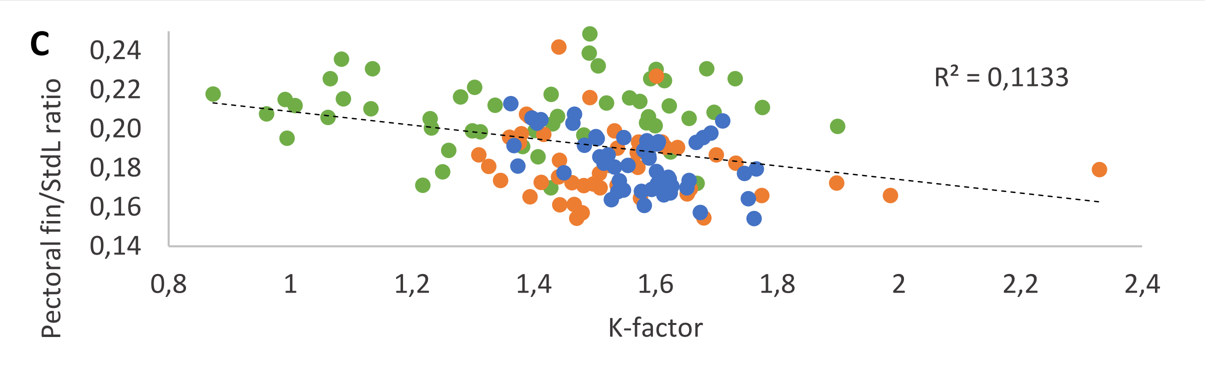

Figure 3.11: The pectoral fin ratio for the 150 fish compared to A: body weight, B: standard length, and C: K-factor.

3.4 Using non-stereo images and their morphometrics to identify sexual mature salmon

3.4.1 Identifying sexually mature salmon based on non-stereo images

Sexually mature salmon have a green/yellow color with red spots and a more rectangular shape, compared to the silver/white colored immature salmon with black spots (Fig. 3.12). The upper jaw is visibly larger for the sexually mature salmon.

Immature salmon showed on average (n=50) to be significantly heavier ($p=0.03$) compared to sexually mature salmon (n=50, Table 3.4), while the mean standard length showed to be insignificantly different ($p=0.67$, Table 3.4). The immature fish had a larger variation in sizes compared to the sexually mature fish upon harvest (Fig. 3.13A-B, Table 3.4). The head size ($p<0.001$) and eye diameter ($p=0.01$) showed to be significantly larger for a sexually mature salmon compared to immature salmon (Table 3.4). The body heights (BHC and BHA) for a sexually mature salmon showed values displaying a more rectangular form than for the immature salmon, as the difference between the BHC and BHA for mature salmon were smaller (Table 3.4). Also, the mature salmon consisted only of male salmon, while the immature salmon consisted of 20 males (mean weight: 5906g) and 28 females (mean weight: 4339g).

Figure 3.12: Close-up image of A: a sexually mature and B: an immature salmon upon harvest.

Table 3.4: The mean weight and ImageJ morphometrics of sexually mature and immature salmon taken upon harvest, where the morphometrics were standard length, body height central, body height anal, eye diameter, snout-pectoral fin, snout-operculum, and upper jaw.

Morphometrics	Sexually mature salmon	Morphometrics /StdL	Immature salmon	Morphometrics /StdL
Weight (g ± SD)	4234 ± 1236		4995 ± 2352	
Standard length (cm ± SD)	67.0 ± 6		68.0 ± 11	
Body height central (cm ± SD)	18.6 ± 2.4	0.28	19.2 ± 4.1	0.28
Body height anal (cm ± SD)	13.6 ± 1.8	0.20	13.1 ± 2.5	0.19
Eye diameter (cm ± SD)	1.4 ± 0.2	0.02	1.2 ± 0.2	0.02
Snout to pectoral fin (cm ± SD)	14.9 ± 1.6	0.22	11.8 ± 1.6	0.18
Snout to operculum (cm ± SD)	14.9 ± 1.5	0.22	11.6 ± 1.6	0.17
Upper jaw (cm ± SD)	7.6 ± 1.1	0.11	5.1 ± 0.8	0.08

3.4.2 Analysis of the BHC and BHA measurement

The difference between BHC and BHA ratio for the sexually mature (diff:0.08) and immature salmon (diff:0.09) showed to be significantly different ($p<0.001$), and that the sexually mature salmon had a more rectangular shape than the immature salmon (Table 3.4). For the BHC ratio there was a positive correlation with the weight (cor.=0.50, cor.=0.62, Fig. 3.13A), standard length (cor.=0.20, cor.=0.46, Fig. 3.13B) and condition factor (cor.=0.69, cor.=0.78, Fig. 3.13C) for the sexually mature and immature salmon respectively. There was also a significant correlation ($p<0.001$) between the BHC ratio and the weight, standard length, and condition factor for the sexually mature and immature salmon, except between the sexually mature salmon and the standard length ($p=0.19$, Fig. 3.13B). For the BHA ratio there was a significant correlation for both groups compared to weight (mature: cor.=0.30, immature: cor.=0.40, $p<0.05$, Fig. 3.13D) and condition factor (mature: cor.=0.56, immature: cor.=0.70, $p<0.001$, Fig. 3.13F). There was no significant correlation between the BHA ratio and the standard length for both groups (mature: cor.=0.02, $p=0.87$; immature: cor.=0.27, $p=0.05$, Fig. 3.13E). The BHC and BHA ratio increased with the size of the salmon (Fig 3.13), and showed that there was no significant difference between the sexually mature and immature salmon for the BHC ($p=0.22$) or the BHA ($p=0.32$) ratio (Table 3.4).

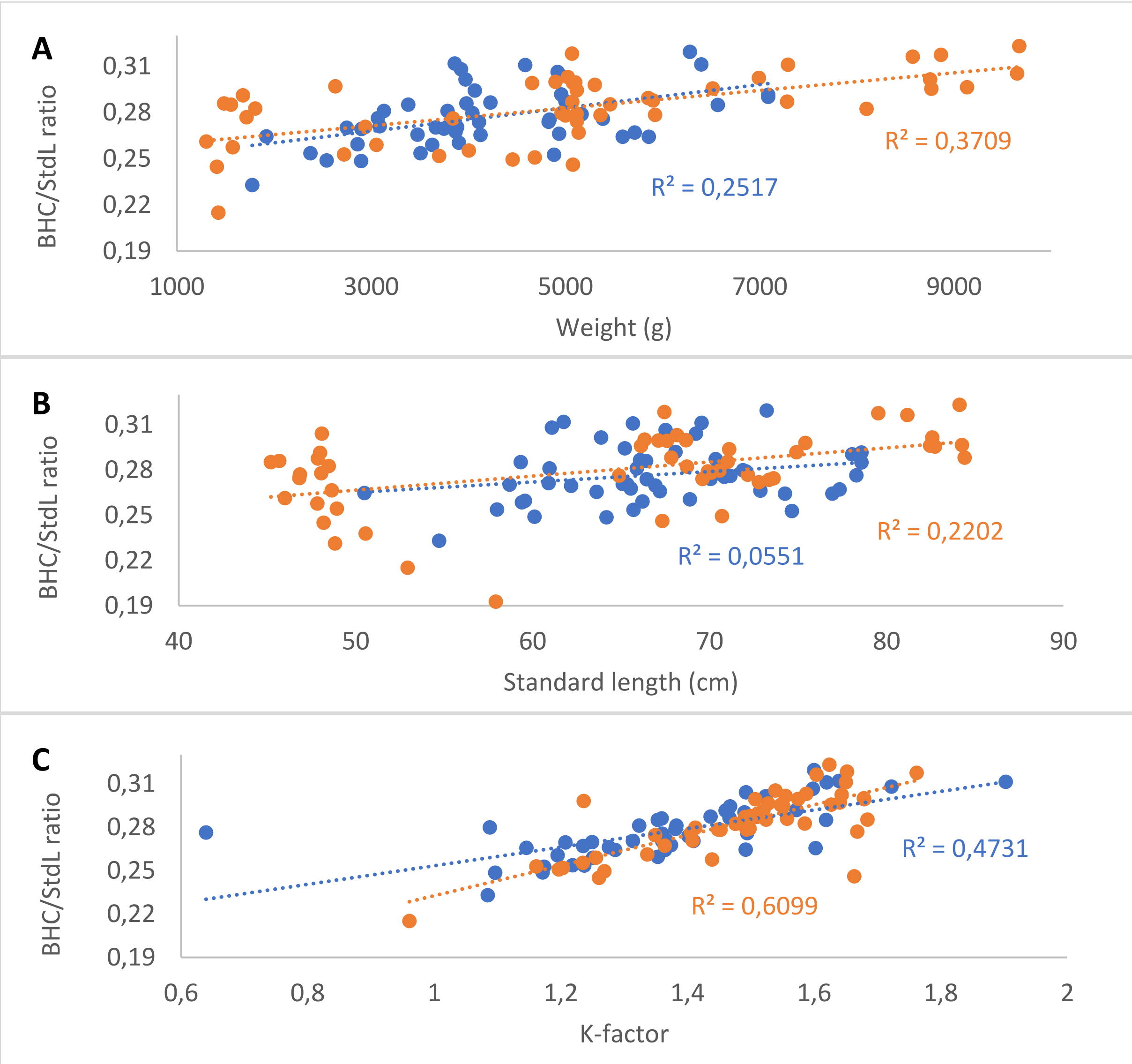

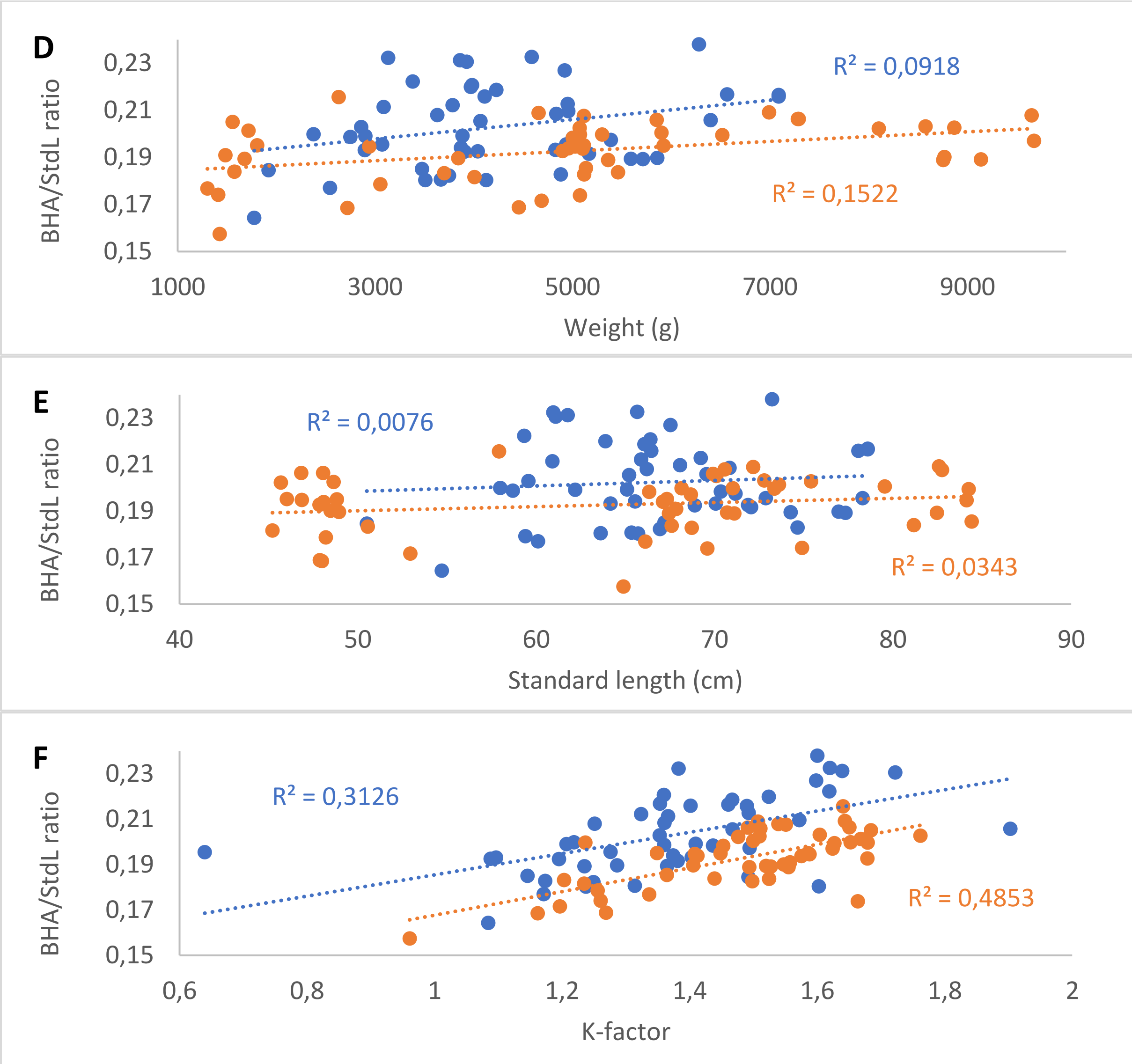

Figure 3.13: Morphometrical measurements of the BHC and BHA for sexually mature (blue) and immature salmon (orange). BHC ratio compared to A: body weight, B: standard length, C: K-factor and BHA ratio compared to D: body weight, E: standard length, and F: K-factor.

3.4.4 Analysis of the eye diameter

The mature salmon had larger eyes compared to the immature salmon (Table 3.4), and the eye diameter ratio showed to be significantly smaller for immature salmon compared to mature salmon ($p=0.02$, Table 3.4). The eye diameter ratio showed to be significantly negatively correlated for the sexually mature (cor. W=-0.55, cor. L=-0.66) and immature salmon (cor. W=-0.60, cor. L=-0.68) for the weight ($p<0.001$, Fig. 3.14A) and standard length ($p<0.001$, Fig. 3.14B). For the eye diameter ratio compared to the condition factor there was no significant correlation for both the sexually mature (cor.=0.02, $p=0.89$) and immature salmon (cor.=-0.03, $p=0.82$, Fig. 3.14C).

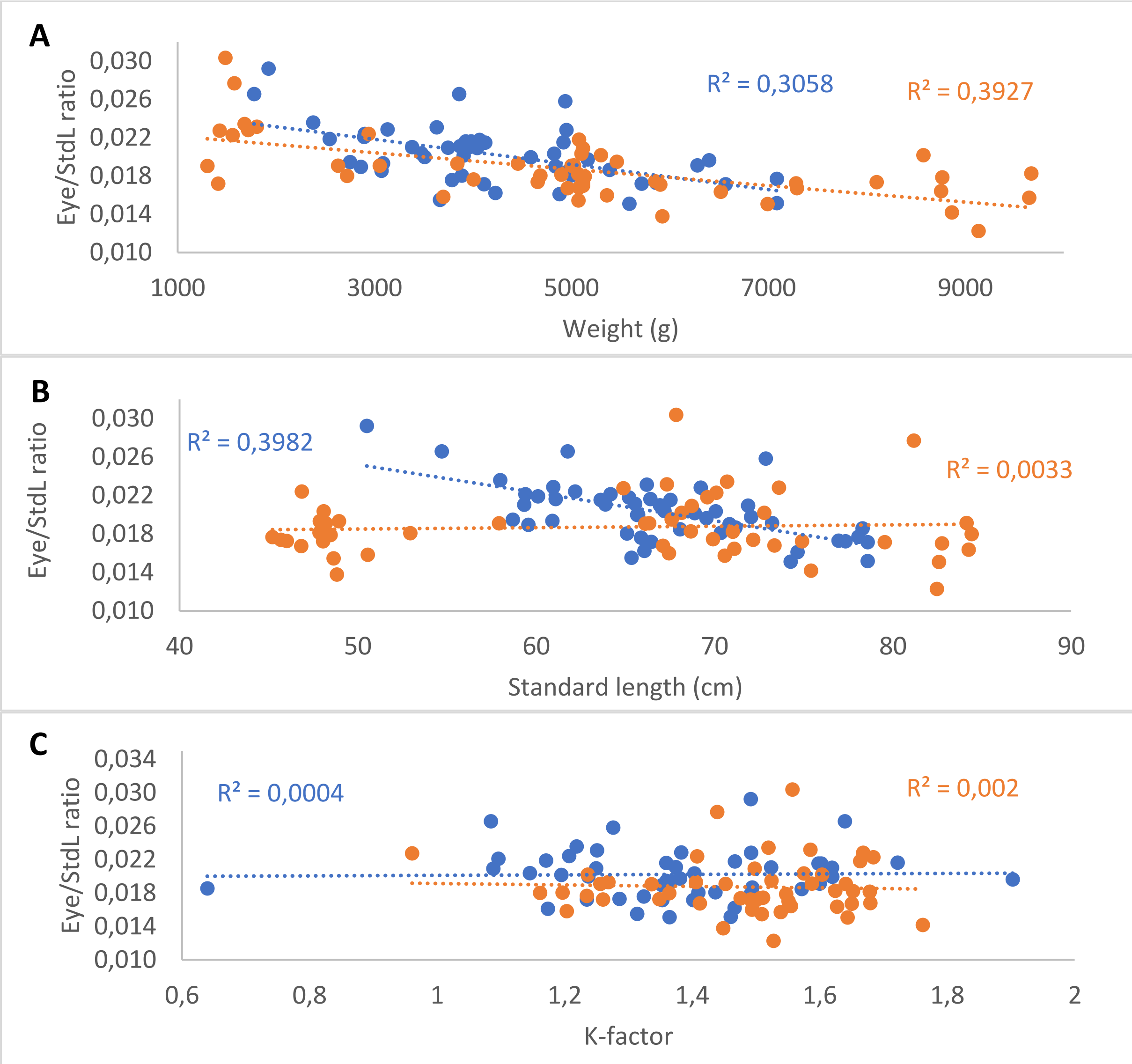

Figure 3.14: Morphometrics of the eye diameter for sexually mature (blue) and immature salmon (orange). The eye diameter ratio compared to A: body weight, B: standard length, and C: K-factor.

3.4.5 Analysis of the head size

The head size was confirmed to be larger for sexually mature salmon than immature salmon (ref. 3.4.2, Table. 3.4), and the clear difference between the head ratios ($p<0.001$) were shown (Fig. 3.15). Both the snout-pectoral fin length and pectoral fin ratio were larger for sexually mature salmon compared to immature salmon (Table 3.4). The upper jaw compared to the snout-pectoral fin length for the two groups of salmon showed to have a significant difference ($p<0.001$) in means. The sexually mature salmon had a longer upper jaw compared to the snout-pectoral fin length than immature salmon, and even though the difference between the upper jaw and snout-pectoral fin varied for each fish, it was overall larger for the sexually mature salmon.

The pectoral fin ratio showed to have a negative correlation with the weight and standard length, and almost no correlation with the condition factor for both the sexually mature (cor. W=-0.27, cor. L=- 0.30, cor. K=-0.09) and immature salmon (cor. W=-0.53, cor. L=-0.64, cor. K=-0.14). There was no significant correlation between the pectoral fin ratio and the condition factor for both groups (mature: p=0.54, immature: p=0.34), nor for the weight for the sexually mature salmon (p=0.07). But there was a significant correlation for the immature salmon compared to weight (p<0.001), and for both groups compared to the standard length (p<0.05). Since all three head measurements were displayed to show the same results (Table 3.4), only the snout-pectoral fin length is displayed in the results section, while the snout-operculum length and upper jaw figures are placed in Appendix D (Fig D.2).

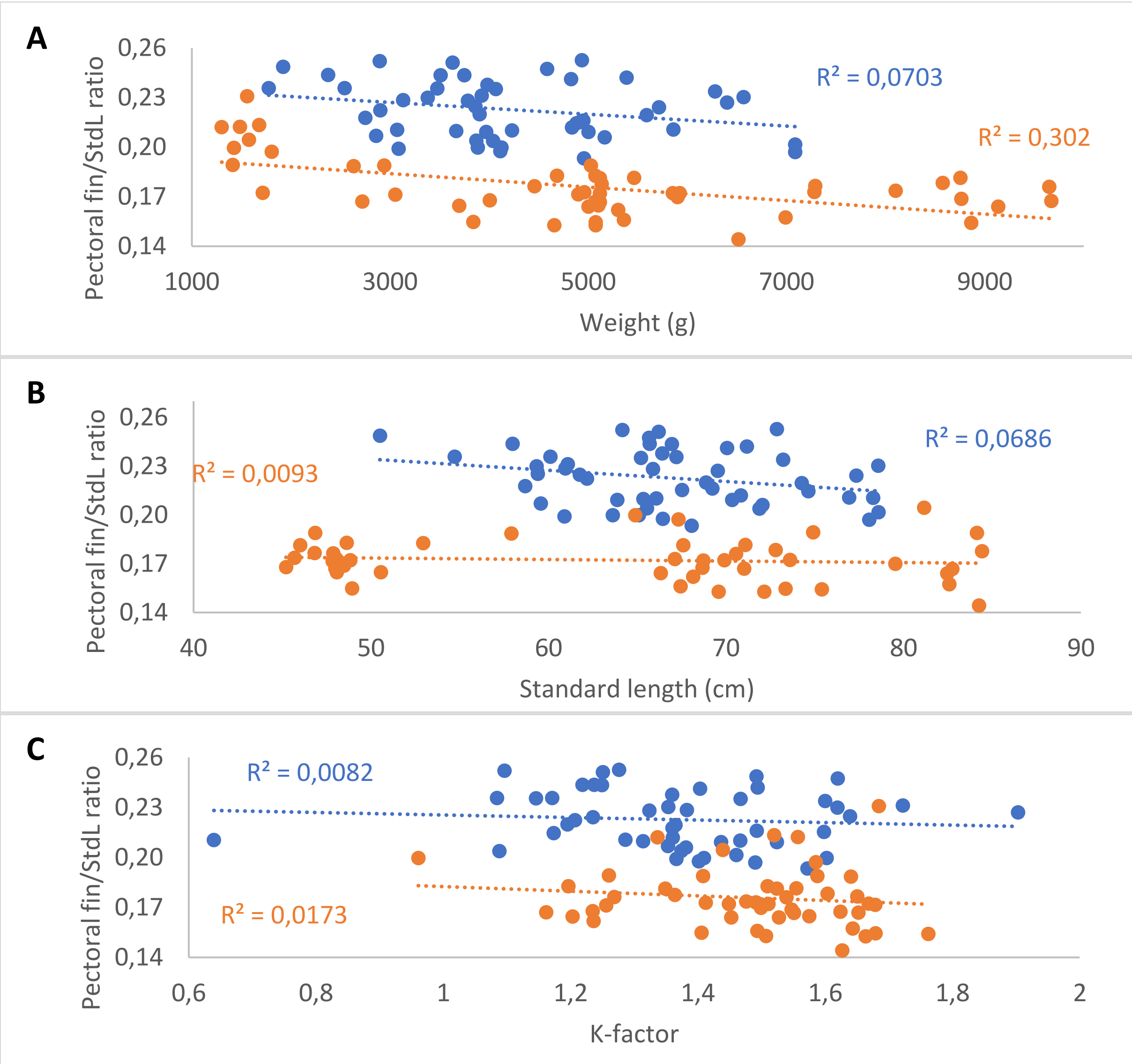

Figure 3.15: Morphometrics of the snout-pectoral fin for sexually mature (blue) and immature salmon (orange). Pectoral fin ratio compared to A: weight, B: standard length, and C: K-factor.

4. Discussion

This study demonstrates that the current use of stereo camera images for estimation of weight distribution in a group of free-swimming sea caged salmon can be highly representative. My data show that the estimated weight correlated well with the manually measured weights. The attempted study of precision in weight estimation of individual free-swimming fish rendered somewhat inconclusive due to a low number of recorded individuals. Detailed analyses of morphometrical relationships in fish of different size classes and sexual maturation status were done to investigate potential for indicators which can be automated in stereo image analysis. The data showed that there is a clear morphometrical difference between the fish of different size, and between sexually mature and immature salmon. This indicates exciting possibilities to use stereo images to explore the morphometric relationships linked with individual fish and sexual maturation status.

4.1 Discussion of methods

4.1.1 Fish material

The fish used in the current study consisted of family groups from a commercial breeding program, and may therefore be more diverse in size compared to standard production fish. Thorland et al. (2020) investigated growth in a very similar composition of a fish group and found genetic variations in growth patterns, which is not investigated or accounted for in the present study. I chose to look at the population as one unit, not taking families into account, and select fish based on how they performed on a populational level. Based on slaughtered weight I chose 150 fish that represented the mean weight and extremes of the population. This was to see the difference in morphometrics and growth between the three size groups.

Selecting fish from e.g. one family would have led to a maximum of 90 fish, and based on which family that were chosen, it could either have over- or underrepresented one group of fish, and thus not being representative for the population. I have not controlled if the genetic growth patterns differ, nor if there are genetic differences in appearances for the 150 selected fish. Investigation of whether family differences exists in the morphometrics was beyond the scope of this study, and the recent study is thus building on the assumption that differences in size is more significant than genetical composition.

One factor that could have affected the growth pattern or morphometrics in this experiment were the detected diseases. The PRV and the CMS both affected the heart and muscles in the farmed salmon (Løvoll *et al.*, 2010; Garseth *et al.*, 2018). Although, I did not investigate how the diseases might have affected growth or morphometrics of the salmon in this thesis, as I had no information about the disease status on an individual level.

4.1.2 Experimental set-up

The experiment which the collected data in this thesis came from, was designed to assess whether there is a scope for selective breeding towards less stress sensitive salmon. Although the stress treatments with CO2 in the freshwater phase and submergence in the early seawater phase had an effect on growth during the periods the fish were exposed to them, they did not affect growth post-stress treatments, i.e. from September 2019-February 2020 in which the growth rate linked with morphometrics at harvest is most relevant for.

The salmon were also treated five times for salmon lice during the experiment. Commercial aquaculture uses delousing on the fish during their production to prevent the lice levels to exceed certain levels. The number of treatments varies a lot with the necessity and the pressure of lice on the farms. There has been done a lot of experiments on the different delousing methods and how this affects the salmon's health, welfare, and growth (Thorstad *et al.*, 2015; Stien *et al.*, 2016; Oppedal *et al.*, 2017; Overton *et al.*, 2019). The manual thermal treatment method used in the current experiment is presumably less invasive than those used in the industry (Folkedal *et al.*, 2021), and are not assumed to have affected growth more than what is normal in commercial aquaculture.

4.1.3 Stereo camera set-up

The position of the antenna fixated in front of the camera was out of position for periods, which caused a great deal of data to be lost. Furthermore, linking PIT identification of individual free-swimming fish in stereo images to the harvest images proved to be difficult, partly due to variating synchronization in time stamp between the two separate logging systems, and partly due to that most images contained several fish overlapping each other. Still, 4 PIT-identified individuals were verified with manual recognition of pigmentation spot patterns (Stien *et al.*, 2017). Also, I could for the first time compare a known size with a size estimated based on a stereo image of an individual free-swimming salmon from a sea cage, which provided a rough estimate of the precision on an individual level.

4.1.4 Representative imaging of fish

Estimation of size distribution within groups of sea caged salmon requires consideration of the fish behavior, and the positioning of the camera. Based on manual observation using sub-surface cameras, the fish did not seem to avoid the stereo camera at any time, which was confirmed by the entire population being represented in the estimated weight distribution. The difference in depths between the size groups must be taken into consideration when taking images of the fish, as smaller fish has shown to position themselves at more shallow depths than larger salmon (Folkedal *et al.*, 2012). Having the camera positioned at one depth may capture images of the mean population, but might not capture the most extreme fish, as for instance loser fish or sick fish might not stay where the camera was positioned, thus, being underestimated. This might be the reason why the estimated weights in February 2020 had a right-shifted distribution compared to the manual sampling. The camera was also supplemented with LED-lamps to receive clear and good quality images throughout the day and night. Whether there was an effect of artificial light on fish behavior on the vertical distribution was not assessed, and could be a topic for future research since caged salmon are attracted to the depth of artificial light at nighttime (Wright *et al.*, 2015).

4.1.5 Ethical considerations

One of the main concerns in commercial aquaculture is the high mortality rates, which was 35% in our experiment. This is a rather high number and may raise ethical concerns. Although, similar rates are found in the industry when fish suffer from disease, and multiple handling and lice treatments (Stien *et al.*, 2019). The handling to facilitate manual sizing of fish is indeed stressful, whereas in this case needed for multiple research purposes. Testing of non-invasive methods for acquiring similar data, as here represented by stereo images, should be considered as great use of the current experimental setup. This will aid in more welfare friendly methods for future use, and importantly, methods which do not interfere with experimental treatments effects as manual sizing might do.

4.1.6 Statistical methods

4.1.6.1 Statistical analysis of stereo camera images of the population from the sea cage

A Welch two sample t-test was used to compare the means of the estimated and manual weights because the number of recordings differed between the two groups, as the estimated recording consisted of weights from 13000-37000 images compared to the 2700-3500 manual weight recordings. The F-test and t-tests does not require a balanced amount of data point to be able to compare them.

For the harvest images for the population and the 150 selected fish, a paired t-test was used as the estimated and real weight of the same individual was compared to each other. A paired t-test was used as it detects small differences in the data compared to a Welch two sample t-test, and is not just based on the mean weight.

4.1.6.2 Statistical analysis of the 150 selected fish and the comparison to the entire population

A Welch two sample t-test were used to compare the mean weight and mean fork length between the 150 selected fish and the population, as there were only two groups that was being compared to each other.

The Shapiro-Wilk normality test can only be used if there is a large amount of data, as normality tests are sensitive to sample size and small samples often pass the normality test. The Shapiro test showed that some dates were significantly different from a normal distribution. This was due to the extremes (end tails) from the q-q plot differing a little from the reference line, resulting in the Shapiro test, which is a very sensitive test, to show that there was a low correlation, even though the most of the data fell along the reference line. Regardless of the Shapiro test, all manual weight distributions were normally distributed as well as the three estimated weight distributions.

To test the weight distribution for the 150 selected fish that consisted of three different size groups, a one-way ANOVA was used, as it compares two or more groups. The one-way ANOVA was chosen because there was only one variable that was being compared between the three groups, and showed if there was a significant weight difference between the size groups during the different weighings. A Tukey HSD-test was used to see which groups that differed from one another and if there were only a difference between two of the groups or if there was a difference between all groups. The condition factor was tested to see when the correlation between weight and fork length started to differ.

4.1.6.4 Statistical analysis of the morphometrics

A linear model was used, as there was more than one explanatory variable the morphometrics are being compared to. The one-way ANOVA was used as there were three size groups being compared, and then a Tukey HSD-test was used to test which groups that differed from one another. For comparing the head sizes with each other, a paired t-test was used to see the difference between the snout-pectoral fin and upper jaw, and if this varied with the size of the fish. The paired t-test was also used to see how much difference there was between the snout-operculum and snout-pectoral fin for each individual fish. A Welch two sample t-test was used when comparing the weight, standard length and morphometrics between the sexually mature and immature salmon, as there were only two groups being compared.

4.2 Discussion of the results

4.2.1 Does the stereo image analysis provide a precise estimate of weight?

The results showed on a populational level that the weight estimates of the stereo images from the sea cage correlated well with the manual weight recordings for both the September and December 2019 measurement, although the deviation was somewhat higher in February 2020. This strongly indicates that the precision of the stereo image analysis is high, and that the weight estimate is accurate for estimating the mean weight of a population of Atlantic salmon. What is interesting is that they had a difference in variance, but an insignificant difference in means for the September and December distribution. This implies that there was something that had to be different between the manual and estimated weights, which could be explained by the precision on an individual level. Where some of the fish were over- or underestimated for weight resulting in an increased variation, but the mean would still be accurate if there is an equal error in over- and underestimating weight. Nilsson and Folkedal (2019) showed that sampling from a population had a high deviation and was size-biased. This resulted in the estimation of the mean weight to be inaccurate compared to stereo image analysis, which showed to represent the population, and give a precise estimate of the mean weight. Also, another consideration that strengthens the accuracy of the stereo image analysis, was that the weight estimates were done after the manual samplings. The first days after the manual samplings had been done, the fish had a tendency to eat less and may have lost weight (Einen, Waagan and Thomassen, 1998), which could explain the negative deviation from the manual measures that the stereo image analysis estimated in September (-0.89%), and December (-0.45).

There could be several different reasons for the February measurement to overestimate the mean weight of the population. A likely explanation of the deviant weight estimation in February 2020 was that the fish were confirmed to have the diseases PRV and CMS, which could have caused the accuracy to be off, as different diseases have shown to reduce growth and increase the mortality rates in farmed Atlantic salmon (Aunsmo *et al.*, 2010; Løvoll *et al.*, 2010; Garseth *et al.*, 2018). Sick individuals may stop feeding, be more stressed and change their behavior in sea cages (Stien *et al.*, 2013). Therefore, they might not behave as they usually would, staying at other depths (Folkedal *et al.*, 2012). Resulting in the stereo camera not capturing images representing the extremes, but only the mean of the population. Whereas fish that were healthy and large, behaved normally and were overrepresented, which biased the estimated weight distribution. This were shown by fish between 6.4-7.8kg, which had a higher frequency than the manual weighed fish, and smaller fish showed to be underrepresented. Resulting in the whole estimation being skewed towards a higher mean weight for the estimated weights compared to the manual measured weights. Although, removing the recurring registrations lead to the estimated mean weight being precise.

The estimated weight based on stereo image analysis, taken upon harvest of the population, compared to the manual recorded weights, showed a significant difference in individual weights with a paired t-test. Where there was only 27g difference in mean weight, with a mean weight > 5kg, which were less than 1% difference. Again, showing that the mean estimations are highly accurate, but the individual weighings are over- and underestimated. For the fork length measurement there was a significant difference between the estimated and manual measured fork length when paired, where the mean fork length estimations were overestimated with 2cm. The estimated fork length was within 3% of the mean fork length. Both the weight and length measurement would be a great tool for fish farmers to use in commercial sea cages to prevent handling of the fish (Beddow *et al.*, 1996; Li, Hao and Duan, 2020).

On an individual level for the 150 selected fish, the estimated weight based on stereo images from harvest, showed no significant difference when paired with the manual measured weights, and had a difference in mean weight of 25g. This shows that the weight estimates on an individual level < 150 is accurate, but as the n increases and the test gets more power, the individual weights begin to show a significant difference when paired. The estimated fork length for the 150 selected fish showed an overestimation of 2cm when compared to the manual measured fork length, the same as on a populational level. This indicates that the length estimates are highly consistent, and only has to be regulated for 2cm to be able to estimate a precise fork length. For fish farmers the estimation of size is important, as it gives an indication of when to slaughter the fish (Beddow *et al.*, 1996; Li, Hao and Duan, 2020).

Having a precise weight estimate on an individual level is not as important for fish farmers, as it is having a correct estimate of the mean weight of the population. Although, the individual composition, as reflected by the size distribution, shows how different parts of the population are performing. This information is valuable for feeding purposes, e.g. if a sub-group remains small (as accompanied with low condition factor) as it is not feeding, and for pre-harvest sale of fish by knowing the proportions of e.g. superior fish.

In other words, the stereo image analysis provided a highly accurate weight estimate on a populational level, where the individual weight estimations, with n > 150, had a systematic error of over- or underestimating weight. A systematic error of overestimating length was found on both an individual and populational level.

4.2.2 Does morphometrical relationship upon harvest represent differences in growth performances?

From the weight distribution of the 150 fish and the population, there was already a significant difference between the three weight groups from the first weighing, even though they partly overlapped during the first and second weighing. This indicates that on an individual level there is not a certainty that the fish of a particular size, will maintain its rank in the size distribution upon harvest. As shown by Thorland et al. (2020), this can partly be explained by a genetical growth difference between individuals. If stereo images show a clear difference between the three groups morphometrics at a mean weight ~50g, there could be a possibility to predict which size the fish would end up with, though this would need further research.

While the condition factor in January 2019 was found to differ between the three groups, the small and medium fish showed to have no difference in condition factor. It is interesting that the medium fish went from having the same condition factor as the small in January to have the same condition as the large in both September and December, before having a lower condition upon harvest. This could be explained by the large fish growing better during the last period and ending up as the largest fish. As for the fork length, there was no difference until January 2019, the same date the condition factor showed to be significant. The condition factor takes both weight and fork length into consideration, and as the weight was significant from the first weighing one would assume that the condition also would be significant, which it was not. This indicates that the fork length might have a larger impact on the condition factor than weight.

The smallest group of fish were picked based on the lowest weight at harvest, where one would assume this is either loser fish, that is slim, or fish that have not been growing well. Some of the smaller fish even had a negative SGR during the last period from December 2019 until February 2020, and the mean SGR were quite low compared to the other two groups of fish. Regardless of this, the smallest fish had a high mean condition factor upon harvest, being 1.37. The condition factor is a variable and changes with both life stage and season, which makes it difficult to define exact values that indicates reduced welfare, but a condition < 0.9 usually indicates emaciation (Stien *et al.*, 2013; Noble *et al.*, 2018). There were only 5 fish showed to be below 1, and about half of the smallest fish showed to have the same condition factor as the medium and large fish.

The largest and smallest fish had a bad correlation with the harvest weight during the first 4 weighings, only the medium fish showed to have a positive correlation with the harvest weight throughout the entire experiment. This might also be due to the medium fish continuously having the mean weight of the population. The largest and smallest fish might have a correlation with the harvest weight during the September and December weighing, due to the fish showing a substantial size gap at this point, that represented the size category the fish upheld until harvest.

The huge weight gain difference between the three size groups was substantial, and something to take into consideration. The largest fish gained almost ten times the weight of the smallest fish during the last period (2 months), showing that the growth development varies, and is highly important for the resulting end weight. The difference in tail length varied with the size of the fish, showing that larger fish had a longer tail length, and that the tail length constituted to a lower percent of its fork length, compared to smaller fish. The largest fish consisted mainly of males (44/50), which correlates well with earlier studies of a population, showing that males were larger than females already at a mean weight of 500g (Thorland *et al.*, 2020).

Body height central and body height anal

The body height of fish compared to its length is practically another form for measuring the condition factor. The positive correlation between BHC ratio and standard length, as well as weight, tells us that the condition factor of the fish increases with size. The longer the fish gets, the more weight it can gain. Larger salmon deposits more fat in their muscles (Torrissen *et al.*, 2011), and expand across the dorsoventral axis, which is why the BHC is largest for the heaviest fish. The same positive correlation is seen for the BHA. Being able to constantly measure the body heights, and comparing them to each other, would enable fish farmers to use these measurements to estimate the growth potential in terms of weight, similar to condition factor.

Eye diameter

Although, the eye diameter increased with the size of the fish, the relative eye size was negatively correlated to body size. Devlin et al. (2012) found out that salmonids with accelerated growth had smaller eyes compared to wild salmonids of the same size, and as the development of the body size increased, the eye diameter continued to have a negative allometric relationship. This is in line with my results. Thus, the eye diameter could be a good indicator for detecting growth performance in commercial aquaculture and to predict the size of the fish. Fish with a small eye diameter but a large eye ratio, could indicate that the fish is small and vice versa.

Head size

From the head size we can see for all three measurements, that there is a negative allometric relationship, where the relative head size decreases with the size of the fish. The longer and heavier the fish, the smaller the head ratio compared to its body size, but the length of the head increases as the size of the fish increases. The snout-pectoral fin measurement was used as the measuring point. Using the snout-operculum length as done by Kadri *et al.* (1997) could pose as a problem, as operculum movement occurs during breathing, or the operculum could be abbreviated. The upper jaw length showed to grow independent of the head size, where the largest fish showed to have the longest upper jaw length, and the smallest fish showed to have the highest upper jaw/standard length ratio. This indicates that the length of the upper jaw could be used as an indicator of the fish size along with the snout-pectoral fin, as the length of both measurements increases as the size of the fish increases. If the head size is large but the ratio is low compared to the size of the fish, this would strongly indicate that the fish is large and vice versa for a small fish. It is easier to measure length and body height for estimating fish size, but relatively to head size this could have some biological consequences. For instance, a young and old fish with the same length and weight, might have different head sizes, which could say something about their growth performance. Thus, using the head size for displaying differences in growth performance, or size of the fish, would be a great tool for fish farmers in commercial aquaculture. Also, if the camera technology could be implemented to constantly measure the head size, the fish farmers would have a great indicator of the fish sizes in the sea cage. This is particularly important in images where the fish overlap from the view of the camera, making it difficult to capture the full body of individuals.

In summary, there was a substantial difference between the morphometrics in both length and ratio upon harvest, which did reflect different growth performances between the three size groups.

4.2.3 Can novel morphometrical relationships reflect if a salmon is sexually mature?

Based on the non-stereo images there is a clear difference of the color, shape, and the head size between a mature and immature salmon. Fish farmers would like to know when a salmon is about to mature and not when it is already mature. Although, for pre-harvest sale of fish, estimation of the number of mature fish would enable these to be removed from the calculation. Based on the measurements done in ImageJ, there is a clear difference between the two groups for the BHA, head size and eye diameter, both in length and ratio. The immature salmon were randomly selected and showed to be significantly larger than sexually mature salmon in weight, which could be explained by maturing fish stopping to eat and allocate bodily resources to the maturation process (Oppedal *et al.*, 2003). Although, they have shown to eat a lot prior to maturation to fill up their reserves before maturing, as it has shown to be an energy draining process (Fleming, 1998; Jonsson and Jonsson, 2009). Another interesting aspect was that the sexually mature salmon only consisted of males, and males have shown to maturate before females in aquaculture (Oppedal *et al.*, 2003). The salmon in the immature control group consisted of 20 males and 28 females, and the males showed to have a much higher mean weight, again proving that males tend to become larger than females (Thorland *et al.*, 2020).

Body height central and body height anal

The BHC ratio showed on average to be equal between sexually mature and immature salmon, while the BHA ratio showed to be larger for sexually mature salmon. The difference between the body height central and the body height anal were significantly smaller for sexually mature than for immature salmon, giving the sexually mature fish a more rectangular shape. Thus, when monitoring salmon, and the ratio between BHC and BHA starts to decrease, this could be used as an indicator that the salmon is starting to mature. Implementing this feature into the stereo image analysis, could help fish farmers to be on alert if the fish starts to change shape. Other possible indicators, such as change of color and head size (Kadri *et al.*, 1997) could be added as supporting features.

Eye diameter

The eye diameter length and eye diameter ratio were larger for sexually mature compared to immature salmon. For the eye diameter ratio compared to standard length, only the mature salmon showed to have a negative allometric correlation, while the immature salmon displayed to have a slight increase. This could be due to the size diversity being narrower for sexually mature salmon than it was for immature salmon, as the immature salmon consisted of sizes varying from 1200-9000g, and the sexually mature salmon only varied from 1700-7000g. Using the eye diameter to measure when a fish is maturing, could be possible, as both the eye diameter length and eye diameter ratio was larger for a maturing fish.

Head size

There was a clear difference between the head size for the two groups, where the sexually mature salmon had a head almost 1/3 larger than immature salmon. Both the head ratio and head length for all three measurements showed to be larger for sexually mature salmon. Sexually mature salmon showed to have snout-pectoral fin ratios above 0.2, while immature salmon showed to have snout-pectoral fin ratios below 0.2. If the snout-pectoral fin ratio starts to move towards or exceed 0.2, there is a strong possibility that this salmon is maturing. The same difference is seen for the upper jaw, and if the upper jaw ratio starts to exceed or move towards 0.1, the salmon is by a high possibility maturing. This indicates a potential in detecting early maturation by constantly monitoring the head to body size ratio.

In summary, there was a significant difference between the morphometrics of sexually mature and immature salmon. The color, BHC/BHA relationship, and head size were clear indicators that separated the two groups.

4.3 Conclusion

The fish size estimation based on stereo image analysis of the free-swimming fish proved to be highly accurate in reflecting the true size distribution of the population, where a skewed estimation before harvest is considered to be caused by altered fish behavior with starvation and disease.

Using images taken by the stereo camera to measure different morphometrical relationships in individual salmon showed that there is a clear difference between the head size, body size, and eyes for different size classes of salmon at harvest. Larger salmon had longer lengths for all measurements, but lower ratios compared to its standard length for the eye diameter and head size. This strongly suggest that if the ratio of the head and eye diameter compared to a salmon’s standard length is low, the fish has had a high growth rate. Morphometrics of the salmon head can thus be used for assessment of growth performance, and has an advantage versus assessment methods, which requires observation of the full fish body. This can be restricted in images of schooling salmon.

The differences in morphometrics between mature and immature salmon proved to be substantial, and several ratios may be used for identifying when a salmon is maturing and to confirm that a salmon is sexually mature. Mature salmon has a relatively larger eye diameter compared with immature salmon, as well as a lower difference between the BHC and BHA, giving the fish a more rectangular shape. The head size was the clearest indicator, as maturing salmon had ratios above 0.2 for the snout-pectoral fin length, and 0.1 for the upper jaw. In conclusion, using those indicators should verify that a salmon is mature. Implementing this into tailored algorithms when analyzing stereo images, should enable detection of early maturation, which should be highly valuable information for fish farmers.

4.4 Future experiments

Future research should investigate the precision and accuracy of stereo image size estimation over full production cycles of salmon, and use multiple cameras at different depths to account for potential depth segregation of fish with different size or health status. A different and perhaps better method would be to vertically profile the cage using one stereo camera to capture the full dynamics. Further testing and improvement of the algorithm for the fork length estimation must be done, to enable correct input for measuring the ratios investigated in this thesis and for correct input for measuring condition factor of fish.

The possibilities for use of stereo camera and stereo image analysis in aquaculture are endless, and if the algorithms are useful in targeting desired morphometrics, advanced assessment of fish welfare evaluation can be carried out without having to remove the fish from the sea cage. Images could be taken continuously and track the fish welfare, and thus provide the fish farmer with historic and online fish status. Substantial research efforts are needed to enable and verify these features.

A problem when observing schooling salmon is that fish are overlapping in images, while key features of existing analyses rely on a full body view. This thesis shows a potential in using only the morphometrics of the head for estimation of fish size, which should be further investigated on a continuous size scale within fish groups as they grow over the full production cycle. The use of stereo image analysis could also be implemented to analyze wild salmonids in rivers, to potentially differentiate the wild and the escaped farmed salmon.

The morphometrics for wild salmon might be different from farmed salmon for both size and age. So, applying this could potentially enable us to analyze the life history of the wild fish, and be able to discriminate them from farmed salmon, as some key morphometrics are described in this study.

Using the morphometrical relationships found in this thesis for detection of sexual maturation in salmon could be supported by other traits such as well-known changes in skin color. Studies are needed to verify the order of when visible changes to the body occur during the maturation process, and thus, which of the candidate indicators that will be most relevant. An additional indicator to support maturation could be arrested growth, which would require tracking the growth history for individual fish. Thus, comparison of these indicators should enable detection of early maturation.

Bibliography

Aksnes, A., Gjerde, B. and Roald, S. O. (1986) ‘Biological, chemical and organoleptic changes during maturation of farmed Atlantic salmon, Salmo salar’, *Aquaculture*. Elsevier, 53(1), pp. 7–20. doi: 10.1016/0044-8486(86)90295-4.

Ang, K. P. and Petrell, R. J. (1997) ‘Control of feed dispensation in seacages using underwater video monitoring: Effects on growth and food conversion’, *Aquacultural Engineering*. Elsevier, 16(1–2), pp. 45–62. doi: 10.1016/S0144-8609(96)01012-6.

Asche, F., Cojocaru, A. L. and Roth, B. (2018) ‘The development of large scale aquaculture production: A comparison of the supply chains for chicken and salmon’, *Aquaculture*. Elsevier B.V., 493, pp. 446–455. doi: 10.1016/j.aquaculture.2016.10.031.

Assefa, A. and Abunna, F. (2018) ‘Maintenance of Fish Health in Aquaculture: Review of Epidemiological Approaches for Prevention and Control of Infectious Disease of Fish’. doi: 10.1155/2018/5432497.

Aunsmo, A. *et al.* (2010) ‘Stochastic modelling of direct costs of pancreas disease (PD) in Norwegian farmed Atlantic salmon (Salmo salar L.)’, *Preventive Veterinary Medicine*. Elsevier, 93(2–3), pp. 233–241. doi: 10.1016/j.prevetmed.2009.10.001.

Aunsmo, A. *et al.* (2014) ‘Field validation of growth models used in Atlantic salmon farming’, *Aquaculture*. Elsevier, 428–429, pp. 249–257. doi: 10.1016/J.AQUACULTURE.2014.03.007.

Aunsmo, A., Skjerve, E. and Midtlyng, P. J. (2013) ‘Accuracy and precision of harvest stock estimation in Atlantic salmon farming’, *Aquaculture*. Elsevier, 396–399, pp. 113–118. doi: 10.1016/j.aquaculture.2013.03.001.

Beddow, T. A. and Ross, L. G. (1996) ‘Predicting biomass of Atlantic salmon from morphometric lateral measurements’, *Journal of Fish Biology*. Wiley, 49(3), pp. 469–482. doi: 10.1111/j.1095-8649.1996.tb00042.x.

Beddow, T. A., Ross, L. G. and Marchant, J. A. (1996) ‘Predicting salmon biomass remotely using a digital stereo-imaging technique’, *Aquaculture*. Elsevier B.V., 146(3–4), pp. 189–203. doi: 10.1016/S0044-8486(96)01384-1.

Bouch, J. (2009) ‘A picture is worth a thousand words’, *Advances in Psychiatric Treatment*. Cambridge University Press, p. 81. doi: 10.1192/apt.15.2.81.

Costa, C. *et al.* (2006) ‘Extracting fish size using dual underwater cameras’, *Aquacultural Engineering*. Elsevier, 35(3), pp. 218–227. doi: 10.1016/j.aquaeng.2006.02.003.

Costello, M. J. (2009) ‘How sea lice from salmon farms may cause wild salmonid declines in Europe and North America and be a threat to fishes elsewhere’, *Proceedings of the Royal Society B: Biological Sciences*. Royal Society, pp. 3385–3394. doi: 10.1098/rspb.2009.0771.

Devlin, R. H. *et al.* (2012) ‘Genetically modified growth affects allometry of eye and brain in salmonids’, *Canadian Journal of Zoology*. NRC Research Press , 90(2), pp. 193–202. doi: 10.1139/Z11-126.

Einen, O., Waagan, B. and Thomassen, M. S. (1998) ‘Starvation prior to slaughter in Atlantic salmon (Salmo salar): I. Effects on weight loss, body shape, slaughter- and fillet-yield, proximate and fatty acid composition’, *Aquaculture*. Elsevier, 166(1–2), pp. 85–104. doi: 10.1016/S0044-8486(98)00279-8.

Elish, M. C. and Boyd, D. (2018) ‘Situating methods in the magic of Big Data and AI’, *Communication*

Monographs. Routledge, 85(1), pp. 57–80. doi: 10.1080/03637751.2017.1375130.

Endal, H. P. *et al.* (2000) 'Effects of continuous additional light on growth and sexual maturity in Atlantic salmon, Salmo salar, reared in sea cages', *Aquaculture*. Elsevier, 191(4), pp. 337–349. doi: 10.1016/S0044-8486(00)00444-0.

FAO (2020) 'WORLD FISHERIES AND AQUACULTURE THE STATE OF SUSTAINABILITY IN ACTION'. doi: 10.4060/ca9229en.

Fleming, I. A. (1998) *Pattern and variability in the breeding system of Atlantic salmon (Salmo salar), with comparisons to other salmonids*.

Folkedal, O. *et al.* (2012) 'Sea caged Atlantic salmon display size-dependent swimming depth', *Aquatic Living Resources*. EDP Sciences, 25(2), pp. 143–149. doi: 10.1051/alr/2012007.

Folkedal, O. *et al.* (2016) 'Salmon welfare index model 2.0: An extended model for overall welfare assessment of caged Atlantic salmon, based on a review of selected welfare indicators and intended for fish he CephsInAction-COST Action FA1301 View project On-farm evaluation of the Sa', *Animal Welfare*, 25, pp. 135–149. doi: 10.1111/raq.12039.

Folkedal, O., Utskot, S. O. and Nilsson, J. (2021) 'Thermal delousing in anaesthetised small Atlantic salmon (Salmo salar) post-smolts : A case study showing the viability of anaesthesia prior to delousing for improved welfare during treatment for salmon lice', *Animal Welfare*, 30(117–120), p. 4. doi: 10.7120/09627286.30.2.117.

Føre, M. *et al.* (2018) 'Precision fish farming: A new framework to improve production in aquaculture', *Biosystems Engineering*. Academic Press, pp. 176–193. doi: 10.1016/j.biosystemseng.2017.10.014.

Fraser, T. W. K. *et al.* (2020) 'No environmental effect on vaccine-induced reduced growth in Atlantic salmon Salmo salar smolts', *Aquaculture Environment Interactions*. Inter-Research Science Center, 12, pp. 327–338. doi: 10.3354/AEI00367.

Garseth, Å. H. *et al.* (2018) 'Cardiomyopathy syndrome in Atlantic salmon *Salmo salar* L.: A review of the current state of knowledge', *Journal of Fish Diseases*. Blackwell Publishing Ltd, 41(1), pp. 11–26. doi: 10.1111/jfd.12735.

Glover, K. A. *et al.* (2005) 'Variation of Atlantic salmon families (Salmo salar L.) in susceptibility to the sea lice Lepeophtheirus salmonis and Caligus elongatus', *Aquaculture*. Elsevier, 245(1–4), pp. 19–30. doi: 10.1016/j.aquaculture.2004.11.047.

Grefsrud, E. S. *et al.* (2021) *Risikorapport norsk fiskeoppdrett 2021 - risikovurdering | Havforskningsinstituttet*, *Havforskningsinstituttet*. Available at: https://www.hi.no/hi/nettrapporter/rapport-fra-havforskningen-2021-8 (Accessed: 11 March 2021).

Gutierrez, A. P. *et al.* (2014) 'Detection of Quantitative Trait Loci (QTL) Related to Grilsing and Late Sexual Maturation in Atlantic Salmon (Salmo salar)', *Marine Biotechnology*, 16(1), pp. 103–110. doi: 10.1007/s10126-013-9530-3.

Handeland, S. . *et al.* (1998) 'Effects of temperature and salinity on osmoregulation and growth of Atlantic salmon (Salmo salar L.) smolts in seawater', *Aquaculture*. Elsevier, 168(1–4), pp. 289–302. doi: 10.1016/S0044-8486(98)00356-1.

Hao, M., Yu, H. and Li, D. (2016) 'The measurement of fish size by machine vision - A review', in *IFIP Advances in Information and Communication Technology*. Springer New York LLC, pp. 15–32. doi: 10.1007/978-3-319-48354-2_2.

Haugholt, K. H. *et al.* (2010) *EXACTUS Technical report EXACTUS RA 1 T1.1 Technology survey*.

Herbinger, C. M. *et al.* (1999) 'Early growth performance of Atlantic salmon full-sib families reared in single family tanks versus in mixed family tanks', in *Aquaculture*. Elsevier, pp. 105–116. doi: 10.1016/S0044-8486(98)00479-7.

Hersoug, B. (2015) 'The greening of Norwegian salmon production', *Maritime Studies*. Springer Verlag, 14(1), pp. 1–19. doi: 10.1186/s40152-015-0034-9.

Heuch, P. A. *et al.* (2005) 'A review of the Norwegian "National Action Plan Against Salmon Lice on Salmonids": The effect on wild salmonids', *Aquaculture*. Elsevier, 246(1–4), pp. 79–92. doi: 10.1016/j.aquaculture.2004.12.027.

Jansen, P. A. *et al.* (2012) 'Sea lice as a density-dependent constraint to salmonid farming', *Proceedings of the Royal Society B: Biological Sciences*. Royal Society Publishing, 279(1737), pp. 2330–2338. doi: 10.1098/rspb.2012.0084.

Jensen, B. B., Qviller, L. and Toft, N. (2020) 'Spatio-temporal variations in mortality during the seawater production phase of Atlantic salmon (Salmo salar) in Norway', *Journal of Fish Diseases*. Blackwell Publishing Ltd, 43(4), pp. 445–457. doi: 10.1111/jfd.13142.

Jonsson, B. and Jonsson, N. (2009) 'A review of the likely effects of climate change on anadromous Atlantic salmon Salmo salar and brown trout Salmo trutta, with particular reference to water temperature and flow', *Journal of Fish Biology*. John Wiley & Sons, Ltd, pp. 2381–2447. doi: 10.1111/j.1095-8649.2009.02380.x.

Kadri, S. *et al.* (1997) 'Early morphological predictors of maturity in one-sea-winter Atlantic salmon', *Aquaculture International*. Springer Netherlands, 5(1), pp. 41–50. doi: 10.1007/BF02764786.

Leclercq, E. *et al.* (2010) 'Body size dimorphism of sea-reared Atlantic salmon (Salmo salar L.): Implications for the management of sexual maturation and harvest quality', *Aquaculture*. Elsevier, 301(1–4), pp. 47–56. doi: 10.1016/j.aquaculture.2010.01.029.

Lecun, Y., Bengio, Y. and Hinton, G. (2015) 'Deep learning', *Nature*. Nature Publishing Group, pp. 436–444. doi: 10.1038/nature14539.

Li, D., Hao, Y. and Duan, Y. (2020) 'Nonintrusive methods for biomass estimation in aquaculture with emphasis on fish: a review', *Reviews in Aquaculture*. Wiley-Blackwell, 12(3), pp. 1390–1411. doi: 10.1111/raq.12388.

Løvoll, M. *et al.* (2010) 'A novel totivirus and piscine reovirus (PRV) in Atlantic salmon (Salmo salar) with cardiomyopathy syndrome (CMS)', *Virology Journal*. BioMed Central, 7(1), p. 309. doi: 10.1186/1743-422X-7-309.

Macqueen, D. J. *et al.* (2008) 'Temperature until the "eyed stage" of embryogenesis programmes the growth trajectory and muscle phenotype of adult Atlantic salmon', *Biology Letters*. Royal Society, 4(3), pp. 294–298. doi: 10.1098/rsbl.2007.0620.

Misimi, E. *et al.* (2006) 'COMPUTER VISION BASED SORTING OF ATLANTIC SALMON (SALMO SALAR) ACCORDING TO SIZE AND SHAPE', in *Proceedings of the First International Conference on Computer Vision Theory and Applications*. SciTePress - Science and and Technology Publications, pp. 265–270. doi: 10.5220/0001370002650270.

Nærings- og fiskeridepartementet (2020) 'Regjeringen skrur på trafikklyset i havbruksnæringen'. regjeringen.no. Available at: https://www.regjeringen.no/no/aktuelt/regjeringen-skrur-pa-trafikklyset-i-havbruksnaringen/id2688939/ (Accessed: 11 March 2021).

Nilsson, J. *et al.* (2013) 'PIT tagged individual Atlantic salmon registrered at static depth positions in a sea cage: Vertical size stratification and implications for fish sampling', *Aquacultural Engineering*.

Elsevier, 55, pp. 32–36. doi: 10.1016/j.aquaeng.2013.02.001.

Nilsson, J. and Folkedal, O. (2019) ‘Sampling of Atlantic salmon Salmo salar from tanks and sea cages is size-biased’, *Aquaculture*. Elsevier B.V., 502, pp. 272–279. doi: 10.1016/j.aquaculture.2018.12.053.

Noble, C. *et al.* (2018) *Velferdsindikatorer for oppdrettslaks: Hvordan vurdere og dokumentere fiskevelferd*. Available at: www.nofima.no/fishwell (Accessed: 5 March 2020).

Olatunji, O., Akinlabi, S. and Madushele, N. (2020) ‘Application of Artificial Intelligence in the Prediction of Thermal Properties of Biomass’, in *Green Energy and Technology*. Springer, pp. 59–91. doi: 10.1007/978-3-030-38032-8_4.

Olaussen, J. O. (2018) ‘Environmental problems and regulation in the aquaculture industry. Insights from Norway’, *Marine Policy*. Elsevier Ltd, 98, pp. 158–163. doi: 10.1016/j.marpol.2018.08.005.

Oppedal, F. *et al.* (2017) ‘Sea lice infestation levels decrease with deeper “snorkel” barriers in Atlantic salmon sea-cages’, *Pest Management Science*. John Wiley and Sons Ltd, 73(9), pp. 1935–1943. doi: 10.1002/ps.4560.

Oppedal, F. *et al.* (2020) ‘Atlantic salmon cope in submerged cages when given access to an air dome that enables fish to maintain neutral buoyancy’, *Aquaculture*. Elsevier B.V., 525, p. 735286. doi: 10.1016/j.aquaculture.2020.735286.

Oppedal, F., Dempster, T. and Stien, L. H. (2011) ‘Environmental drivers of Atlantic salmon behaviour in sea-cages: A review’, *Aquaculture*. Elsevier, pp. 1–18. doi: 10.1016/j.aquaculture.2010.11.020.

Oppedal, F., Taranger, G. L. and Hansen, T. (2003) ‘Growth performance and sexual maturation in diploid and triploid Atlantic salmon (Salmo salar L.) in seawater tanks exposed to continuous light or simulated natural photoperiod’, *Aquaculture*. Elsevier, 215(1–4), pp. 145–162. doi: 10.1016/S0044-8486(02)00223-5.

Overton, K. *et al.* (2018) ‘The use and effects of hydrogen peroxide on salmon lice and post-smolt Atlantic salmon’, *Aquaculture*. Elsevier B.V., 486, pp. 246–252. doi: 10.1016/j.aquaculture.2017.12.041.

Overton, K. *et al.* (2019) ‘Salmon lice treatments and salmon mortality in Norwegian aquaculture: a review’, *Reviews in Aquaculture*. Wiley-Blackwell, 11(4), pp. 1398–1417. doi: 10.1111/raq.12299.

Pankhurst, N. W. and Montgomery, J. C. (1994) ‘Uncoupling of Visual and Somatic Growth in the Rainbow Trout <i>Oncorhynchus mykiss</i>’, *Brain, Behavior and Evolution*. Karger Publishers, 44(3), pp. 149–155. doi: 10.1159/000113586.

Quinton, C. D., McMillan, I. and Glebe, B. D. (2005) ‘Development of an Atlantic salmon (Salmo salar) genetic improvement program: Genetic parameters of harvest body weight and carcass quality traits estimated with animal models’, in *Aquaculture*. Elsevier, pp. 211–217. doi: 10.1016/j.aquaculture.2005.02.030.

Rottmann, R. W., Francis-Floyd, R. and Durborow, R. (1992) *Southern Regional Aquaculture Center The Role of Stress in Fish Disease*.

Samsing, F. *et al.* (2014) ‘High host densities dilute sea lice Lepeophtheirus salmonis loads on individual Atlantic salmon, but do not reduce lice infection success’, *Aquaculture Environment Interactions*. Inter-Research, 6(1), pp. 81–89. doi: 10.3354/aei00118.

Schindelin, J. *et al.* (2015) ‘The ImageJ ecosystem: An open platform for biomedical image analysis’, *Molecular Reproduction and Development*. John Wiley and Sons Inc., 82(7–8), pp. 518–529. doi: 10.1002/mrd.22489.

Schneider, C. A., Rasband, W. S. and Eliceiri, K. W. (2012) 'NIH Image to ImageJ: 25 years of image analysis', *Nature Methods*. Nature Publishing Group, pp. 671–675. doi: 10.1038/nmeth.2089.

Simpson, A. L. (1992) 'Differences in body size and lipid reserves between maturing and nonmaturing Atlantic salmon parr, Salmo salar L.', *Canadian Journal of Zoology*. NRC Research Press Ottawa, Canada , 70(9), pp. 1737–1742. doi: 10.1139/z92-241.

Skretting (2012) *Fôr*. Available at: https://www.skrettingguidelines.com/readimage.aspx?pubid=cd8a45bd-0e6e-409c-a2ee-1da2b7d19b06 (Accessed: 10 March 2021).

Solem, Ø. and Berg, O. K. (2011) 'Morphological differences in parr of Atlantic salmon Salmo salar from three regions in Norway', *Journal of Fish Biology*. John Wiley & Sons, Ltd, 78(5), pp. 1451–1469. doi: 10.1111/j.1095-8649.2011.02950.x.

Solem, Ø., Berg, O. K. and Kjøsnes, A. J. (2006) 'Inter- and intra-population morphological differences between wild and farmed Atlantic salmon juveniles', *Journal of Fish Biology*. John Wiley & Sons, Ltd, 69(5), pp. 1466–1481. doi: 10.1111/j.1095-8649.2006.01208.x.

Stien, L. H. *et al.* (2013) 'Salmon Welfare Index Model (SWIM 1.0): a semantic model for overall welfare assessment of caged Atlantic salmon: review of the selected welfare indicators and model presentation', *Reviews in Aquaculture*. John Wiley & Sons, Ltd, 5(1), pp. 33–57. doi: 10.1111/j.1753-5131.2012.01083.x.

Stien, L. H. *et al.* (2016) '"Snorkel" sea lice barrier technology reduces sea lice loads on harvest-sized Atlantic salmon with minimal welfare impacts', *Aquaculture*. Elsevier B.V., 458, pp. 29–37. doi: 10.1016/j.aquaculture.2016.02.014.

Stien, L. H. *et al.* (2017) 'Consistent melanophore spot patterns allow long-term individual recognition of Atlantic salmon *Salmo salar*', *Journal of Fish Biology*. Blackwell Publishing Ltd, 91(6), pp. 1699–1712. doi: 10.1111/jfb.13491.

Stien, L. H. *et al.* (2019) *Dyrevelferd i norsk fiskeoppdrett*, *Havforskningsinstituttet*. Available at: https://www.hi.no/resources/kunnskapsstatus-risikorapportar/2019/Kap_7_Dyrevelferd-i-norsk-fiskeoppdrett.pdf (Accessed: 24 March 2021).

Stien, L. H., Størkersen, K. V. and Gåsnes, S. K. (2020) *ANALYSE AV DØDELIGHETSDATA FRA SPØRREUNDERSØKELSE OM VELFERD HOS RENSEFISK*.

Taranger, G. L. *et al.* (2010) 'Control of puberty in farmed fish', *General and Comparative Endocrinology*. Academic Press Inc., 165(3), pp. 483–515. doi: 10.1016/j.ygcen.2009.05.004.

Tawalbeh, L. A. *et al.* (2016) 'Mobile Cloud Computing Model and Big Data Analysis for Healthcare Applications', *IEEE Access*. Institute of Electrical and Electronics Engineers Inc., 4, pp. 6171–6180. doi: 10.1109/ACCESS.2016.2613278.

Thorland, I. *et al.* (2020) 'Genetic variation in growth pattern within a population of farmed Atlantic salmon (Salmo salar) during a standard production cycle', *Aquaculture*. Elsevier B.V., 518, p. 734735. doi: 10.1016/j.aquaculture.2019.734735.

Thorstad, E. B. *et al.* (2015) 'Effects of salmon lice Lepeophtheirus salmonis on wild sea trout salmo trutta - A literature review', *Aquaculture Environment Interactions*. Inter-Research, pp. 91–113. doi: 10.3354/aei00142.

Tillett, R. D., Bull, C. R. and Lines, J. A. (1999) 'An optical method for the detection of sea lice, Lepeophtheirus salmonis', *Aquacultural Engineering*. Elsevier, 21(1), pp. 33–48. doi: 10.1016/S0144-8609(99)00022-9.

Torrissen, O. *et al.* (2011) 'Atlantic Salmon (*Salmo salar*): The "Super-Chicken" of the Sea?', *Reviews in Fisheries Science*. Informa UK Limited, 19(3), pp. 257–278. doi: 10.1080/10641262.2011.597890.

Wright, D. *et al.* (2015) 'Atlantic salmon Salmo salar instantaneously follow vertical light movements in sea cages', *Aquaculture Environment Interactions*. Inter-Research, 7(1), pp. 61–65. doi: 10.3354/aei00136.

Appendix

Appendix A: Coding from R

 # Installing the right packages and finding the right files

```
install.packages("fs")
install.packages("readxl")

library(fs)
library(readxl)

Allfisk.df = read_excel("Datamateriale2.xlsx", 1)
fisk150.df = read_excel("Datamateriale.xlsx", 2)
mature.df = read_excel("Datamateriale.xlsx", 3)
weightDigi.df = read_excel("Datamateriale.xlsx", 4)
weight150.df = read_excel("Datamateriale.xlsx", 5)
ABpred.df = read_excel("Datamateriale.xlsx", 6)
```

 # F-test and a paired t-test were used to compare the harvest stereo image estimated weights and fork lengths to the manual size recordings. Welch two sample t-test was used when comparing the estimated weight from the with the manual measured weights

```
var.test(fisk150.df$harvestW, fisk150.df$Pred_weight)

t.test(fisk150.df$harvestW, fisk150.df$Pred_weight, paired = TRUE,
conf.level = 0.95)

t.test(Allfisk.df$new_w, ABpred.df$ABS_w, paired = FALSE, conf.level =
0.95)
```

 # F-test and Welsh two sample t-test for the 150 fish compared to the population for weight and fork length

```
var.test(fisk150.df$harvestW, as.numeric(Allfisk.df$harvestW))

t.test(fisk150.df$harvestW, as.numeric(Allfisk.df$harvestW), paired =
FALSE, var.equal = FALSE, conf.level = 0.95)
```

 # One-way ANOVA and Tukey HSD-test done for both the weight and K-factor for the 150 selected fish

```
Res1.an <- lm(as.numeric(w_jul18) ~ Sizegroup, data = fisk150.df)
anova(res1.an)
res1.an

do.aov1 <- aov(as.numeric(w_jul18) ~ Sizegroup, data=fisk150.df)
summary(do.aov1)
TukeyHSD(do.aov1)
```

 # Checking the correlation between the different morphometrics and the weight, standard length, and K-factor with a Pearson's product-moment correlation test for the 150 selected salmon

```
cor.test(fisk150.df$CentralheightStdLRatio, fisk150.df$harvestW)
```

Linear model, ANOVA and Tukey HSD-test for each response variable

```
lm1 <-  lm(CentralheightStdLRatio ~ harvestW + StdL + K.harv.Stdl +
SGR, data=fisk150.df)
summary(lm1)

do.aov1 <- aov(CentralheightStdLRatio ~ Sizegroup, data=fisk150.df)
summary(do.aov1)
TukeyHSD(do.aov1)
```

F-test and Welch two sample t-test for comparing the weight and standard length between mature and immature salmon

```
Var.test(mature.df$harvestW[mature.df$Sizegroup==”mature”],
mature.df$harvestW[mature.df$Sizegroup==”nonmature”])

t.test(mature.df$harvestW[mature.df$Sizegroup==”mature”],
mature.df$harvestW[mature.df$Sizegroup==”nonmature”], var.equal =
FALSE, paired = FALSE, conf.level = 0.95)
```

Linear model, ANOVA and Tukey HSD-test for each response variable

```
lm7 <-  lm(CentralheightStdLRatio ~ harvestW + StdL + K.harv.Stdl +
SGR, data=mature.df)
summary(lm7)

do.aov7 <- aov(CentralheightStdLRatio~Sizegroup, data=mature.df)
summary(do.aov7)
TukeyHSD(do.aov7)
```

Checking the correlation between the different morphometrics and the weight, standard length, and K-factor with a Pearson’s product-moment correlation test for sexually mature and immature salmon

```
cor.test(mature.df$CentralheightStdLRatio[mature.df$Sizegroup=="mature"
], as.numeric(mature.df$K.harv.Stdl[mature.df$Sizegroup=="mature"]))
```

Appendix B: Data from Aquabyte

Table B.1: The predicted weight and fork length from Aquabyte and the ImageJ standard length, with the manual measured fork length and weight for the 150 fish.

Fish ID	Weight (g)	Fork length (cm)	ImageJ standard length (cm)	Predicted weight (g)	Predicted fork length (cm)
041A47172E	10385	86	89.1	10992	88.9
041A479EFC	10190	84	84.9	9843	86.4
041A4714BC	10045	83	85.6	9285	84.1
041A433DF0	9765	85	85.0	10377	87.6
041A46E223	9672	83	84.1	9261	84.3
041A434043	9650	85	85.6	10637	88.3
041A46CCF3	9635	81	83.1	8883	82.0
041A4734BD	9500	83	83.6	9164	83.7
041A473522	9445	81	81.5	9300	82.7
041A47A475	9220	84	85.0	9007	83.3
041A47A55D	9183	82	82.7	9424	84.9
041A473368	9135	83	84.3	8428	82.7
041A47A7CD	9120	85	86.6	8428	82.7
041A43433C	9110	84	85.7	9169	83.6
041A4347BB	9080	80	81.9	9698	84.6
041A433CD0	9035	79	80.2	8245	79.8
041A433F2D	9030	81	82.4	8781	84.8
041A433FF6	9018	82	83.0	9535	86.0
041A479FDE	9005	80	82.8	8335	82.3
041A433E55	8947	80	80.6	9266	84.7
041A433F69	8945	80	82.6	9167	83.6
041A479EF6	8920	81	81.4	8590	81.9
041A46C7F3	8905	82	81.0	8740	81.9
041A433FC5	8865	79	79.5	7994	79.4
041A471583	8845	85	85.9	8537	83.4
041A43425F	8829	83	84.1	8728	85.2
041A43435E	8819	82	83.6	8719	83.0
041A473404	8815	82	83.2	8822	83.1
041A46C8F7	8765	81	86.3	8778	82.4
041A4734A8	8765	81	82.7	8253	81.7
041A472C63	8755	81	82.6	8514	82.3
041A471607	8745	79	79.1	7954	81.3
041A47A5D5	8718	80	81.6	8734	81.7
041A46E069	8687	81	81.8	8459	80.3
041A433C56	8680	82	82.5	8794	81.9
041A4344F4	8675	82	83.2	8615	81.7
041A4730D1	8650	82	83.9	8463	81.6
041A47A561	8635	81	81.8	8463	81.6
041A479F2C	8630	79	82.5	9244	84.7
041A47A1DA	8612	80	81.2	8790	83.2

041A46E41E	8576	79	81.2	8033	79.3
041A47A5B6	8565	81	82.7	8183	80.5
041A47A6C0	8558	82	85.3	8212	83.4
041A47A491	8540	80	80.7	8317	80.3
041A4713E5	8539	84	85.4	8464	83.5
041A434267	8493	82	84.4	8830	82.9
041A470F6D	8440	79	79.1	8233	80.6
041A471377	8440	80	81.1	8437	82.3
041A47A23D	8436	81	81.3	8422	82.4
041A46EA87	8415	80	82.3	9090	84.0
041A471013	5900	73	73.4	5799	75.4
041A479FE5	5885	70	70.2	5915	73.3
041A4750D1	5833	71	71.8	5704	71.3
041A43405D	5780	70	70.7	6067	74.8
041A43468D	5745	73	73.6	5915	73.7
041A434199	5725	69	70.3	5588	73.2
041A433AA9	5610	73	73.4	5628	73.5
041A47A34D	5590	71	70.9	5449	73.1
041A472F4C	5512	71	72.1	6170	74.6
041A433C18	5460	71	71.0	5312	72.2
041A433B2E	5400	73	72.5	5675	72.8
041A46E70E	5386	71	69.5	5567	70.7
041A472F45	5345	70	71.5	5005	70.4
041A43470B	5345	69	68.6	5437	71.2
041A47A01D	5330	70	68.8	5709	72.9
041A47A4A0	5320	73	73.4	6042	75.6
041A47A3D6	5315	65	64.4	5528	70.8
041A47A4F4	5292	65	65.3	5041	70.8
041A47A421	5265	73	73.8	5617	72.8
041A47A5EF	5260	67	66.7	5598	71.3
041A472DE4	5254	70	70.0	5966	73.4
041A46CE62	5250	72	72.2	5649	75.0
041A4347BF	5246	74	73.4	5598	74.0
041A46E6BC	5245	72	72.8	5330	72.1
041A4345ED	5240	71	71.4	5498	71.7
041A434594	5240	69	69.4	5152	70.1
041A46C773	5240	68	68.8	5242	71.7
041A47A737	5220	70	70.2	5701	74.0
041A46D2BC	5200	69	68.8	5054	70.0
041A47AA85	5195	70	71.2	5510	73.2
041A47A5E0	5184	69	72.2	5041	70.8
041A47A3B7	5180	70	69.6	5573	73.1
041A47A7CF	5143	70	69.4	5064	70.0
041A472E16	5117	70	69.9	5590	72.5
041A46E7C8	5100	70	68.7	4874	69.0
041A46E0A1	5098	71	71.6	5370	71.5

041A46E7CC	5095	69	70.1	5165	69.5
041A47A056	5075	67	67.1	5432	71.6
041A434588	5068	67	67.4	5164	69.6
041A47A680	5046	68	67.8	4900	67.9
041A47A7AB	5025	68	68.1	5122	71.1
041A47A4A9	5015	71	69.7	5153	74.1
041A433B3C	4980	71	70.1	5202	71.5
041A46CFF0	4971	70	71.2	4957	70.5
041A4714E2	4960	70	70.6	5117	72.0
041A433B75	4957	68	68.1	4859	68.2
041A46E803	4956	67	66.3	4694	67.4
041A472F1F	4950	69	69.2	4954	70.5
041A434711	4945	60	59.7	4835	66.0
041A46CABA	4925	71	70.7	4882	72.7
041A47AA8F	2200	52	52.2	2210	57.5
041A472C32	2165	53	53.1	2309	57.4
041A46C8B9	2132	50	51.3	2028	55.7
041A4341E5	2102	53	52.4	2494	57.8
041A4731F5	2050	52	51.9	2211	56.7
041A47A8D3	2048	50	50.4	2291	56.5
041A47A6C7	2030	58	47.7	2247	56.3
041A472B36	2015	55	55.1	2316	57.3
041A472E6B	1932	57	57.9	2232	59.1
041A46CECE	1923	48	48.1	2296	55.4
041A47AA59	1921	52	50.5	1899	54.0
041A471100	1920	48	47.6	2125	54.9
041A472F97	1880	51	51.2	1813	53.4
041A470AAE	1860	48	47.9	1780	52.2
041A472D82	1860	51	50.9	1740	51.5
041A470C1A	1840	53	57.0	1880	55.0
041A47A853	1805	49	48.5	1944	52.8
041A47A8FD	1793	49	49.4	1824	53.4
041A434598	1790	58	48.0	1757	52.0
041A472ABF	1775	55	54.7	1986	57.5
041A434795	1732	49	48.6	1892	53.7
041A47A228	1725	48	47.6	1803	53.6
041A479EE8	1715	46	46.8	1761	53.0
041A47A943	1707	47	46.9	1705	51.3
041A47A5CF	1698	50	49.7	1788	53.9
041A475D9B	1695	58	57.9	1787	57.3
041A479FAA	1695	55	55.2	1932	59.0
041A434581	1690	47	50.5	1796	53.9
041A4729C3	1685	52	51.7	1894	54.4
041A472A1D	1683	50	50.6	1602	52.1
041A46E33D	1680	54	54.1	1657	15.5
041A479DFB	1678	48	48.0	1739	52.0

041A433EFA	1665	47	46.8	1554	49.9
041A47A9A8	1658	52	51.0	1714	54.0
041A47A610	1620	48	48.4	1682	52.6
041A47A2D5	1575	47	47.8	1475	51.7
041A433C7F	1567	52	51.7	1474	51.7
041A479D4D	1556	45	45.2	1687	54.0
041A472FF3	1510	45	45.3	1360	48.7
041A47A48B	1499	48	48.9	1581	51.9
041A4733BF	1484	45	45.7	1479	51.0
041A433C0C	1435	48	48.0	1402	49.9
041A479F90	1425	53	52.9	1554	53.5
041A4344E5	1410	50	48.2	1244	48.5
041A433D1B	1358	48	48.0	1342	49.7
041A47A44C	1336	50	50.1	1431	52.0
041A472F14	1301	46	46.0	1318	49.5
041A43471B	1273	43	43.1	1350	49.0
041A471486	1265	49	48.8	1352	49.8
041A47A116	1262	48	48.1	1238	48.9

Appendix C: Growth development data

Table C.1: Mean weight for the five groups

Fish group	150 fish	Large	Medium	Small	All fish
Date (dd.mm.yyyy)	**Weight (g)**				
31.07.2018	49	54	50	45	59
29.08.2018	71	79	70	64	78
01.10.2018	93	104	91	82	99
22.01.2019	463	560	444	389	449
04.09.2019	2122	3062	2078	1198	2062
02.12.2019	3962	6362	4061	1452	3992
12.02.2020	5362	8969	5405	1712	5408

Table C.2: Mean fork length for the five groups

Fish group	150 fish	Large	Medium	Small	All fish
Date (dd.mm.yyyy)	**Fork length (cm)**				
31.07.2018	15.1	15.5	15.1	14.7	15.0
29.08.2018	17.1	17.7	17.1	16.5	17.0
01.10.2018	19.4	20.2	19.4	18.6	19.3
22.01.2019	33.8	35.8	33.5	32.2	33.3
04.09.2019	54.9	61.9	55.0	47.7	54.7
02.12.2019	62.9	74.9	65.1	48.8	64.2
12.02.2020	67.4	81.6	70.6	50.2	69.8

Table C.3: Mean condition factor for the five different groups

Fish group	150 fish	Large	Medium	Small	All fish
Date (dd.mm.yyyy)	**K-factor**				
31.07.2018	1.4	1.4	1.4	1.4	1.4
29.08.2018	1.4	1.4	1.4	1.4	1.4
01.10.2018	1.3	1.3	1.3	1.3	1.2
22.01.2019	1.2	1.2	1.2	1.2	1.2
04.09.2019	1.2	1.3	1.3	1.1	1.2
02.12.2019	1.4	1.5	1.5	1.2	1.5
12.02.2020	1.5	1.7	1.6	1.4	1.5

Table C.4: Mean SGR for the five different groups

Fish group	150 fish	Large	Medium	Small	All fish
Date (dd.mm.yyyy)	SGR (%/day)				
31.07.2018-29.08.2018	1.3	1.3	1.2	1.2	1.2
29.08.2018-01.10.2018	0.8	0.9	0.8	0.8	0.8
01.10.2018-22.01.2019	1.4	1.5	1.4	1.4	1.4
22.01.2019-04.09.2019	0.7	0.8	0.7	0.4	0.7
04.09.2019-02.12.2019	0.6	0.8	0.8	0.3	0.7
02.12.2019-12.02.2020	0.4	0.5	0.4	0.3	0.4

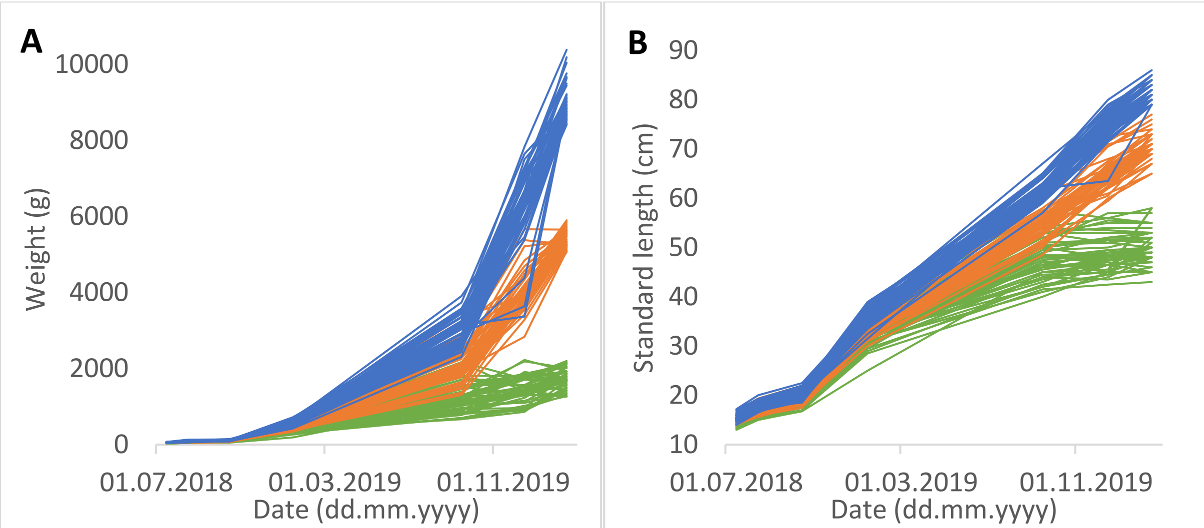

Figure C.1: Growth development for the 150 fish. A: Weight and B: standard length.

Appendix D: Additional morphometrical figures

D.1: Morphometrics of the 150 selected salmon

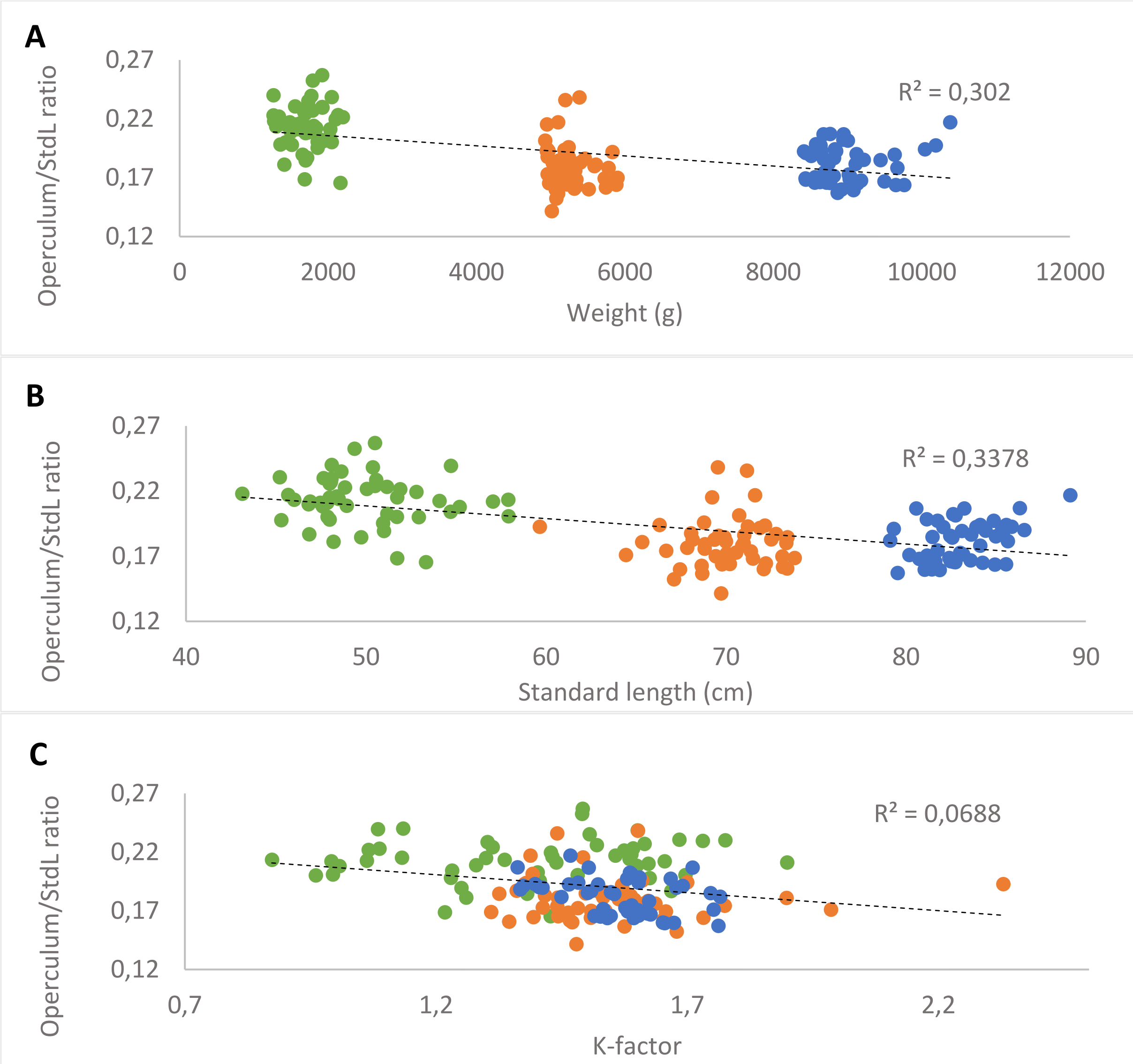

Figure D.1: The snout-operculum ratio for the 150 fish compared to A: body weight, B: standard length and C: K-factor.

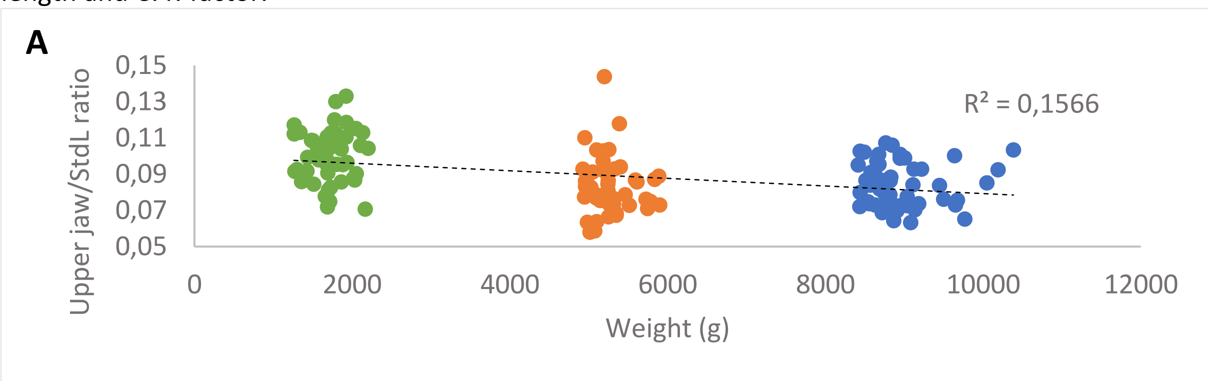

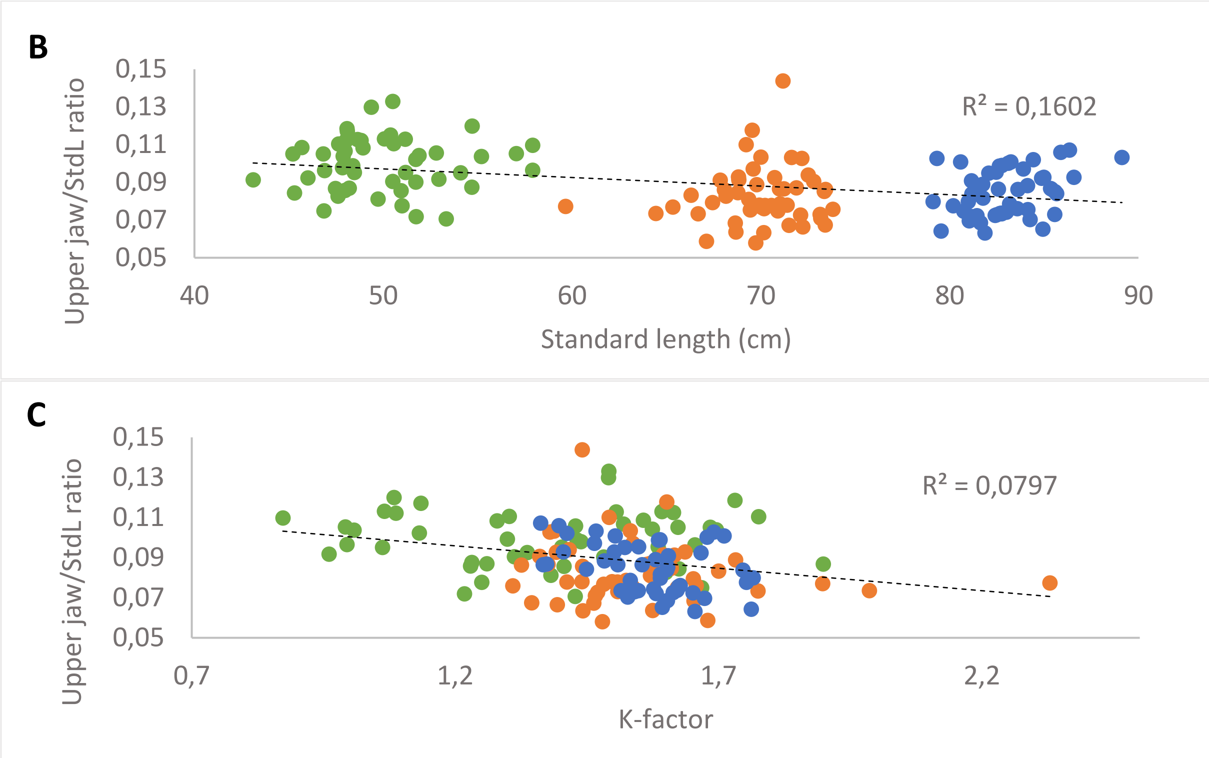

Figure D.1: The upper jaw ratio for the 150 fish compared to A: body weight, B: standard length and C: K-factor.

D.2: Morphometrics of the selected mature and immature salmon

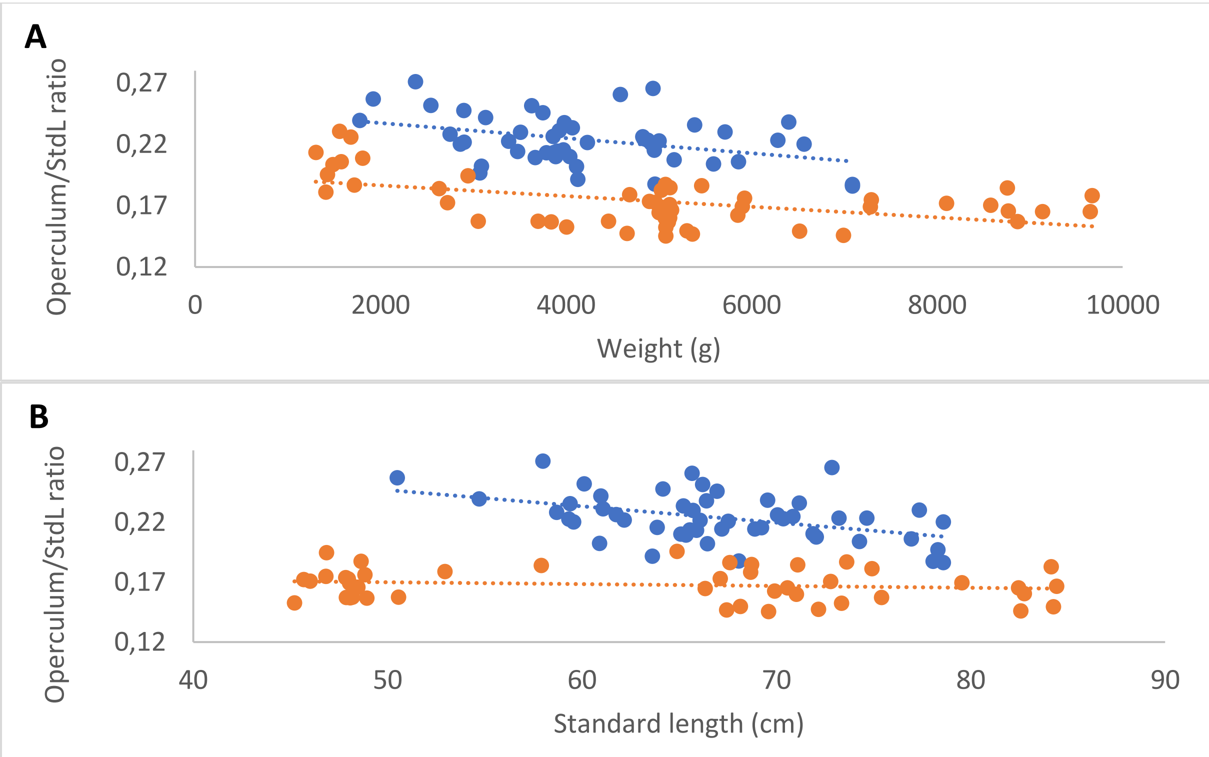

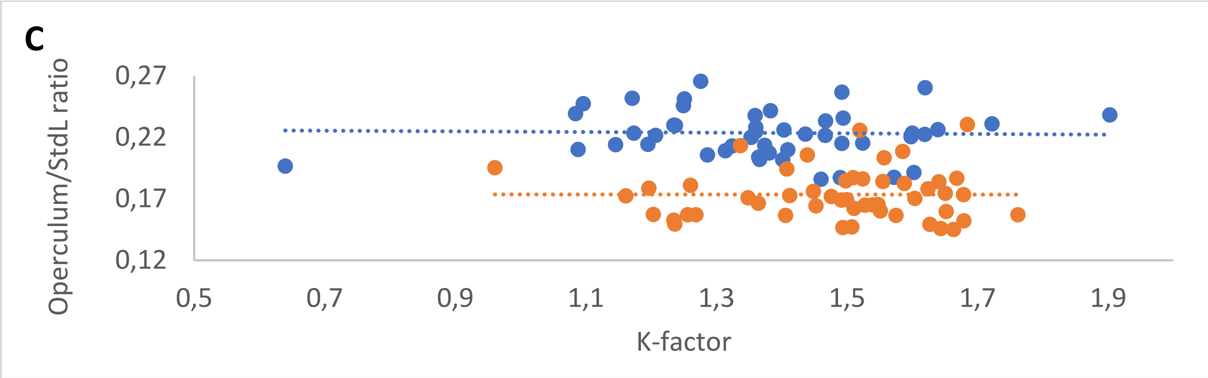

Figure D.1: Morphometrics of the snout-operculum for sexually mature (blue) and immature salmon (orange). Snout-operculum ratio compared to A: weight, B: standard length and C: K-factor.

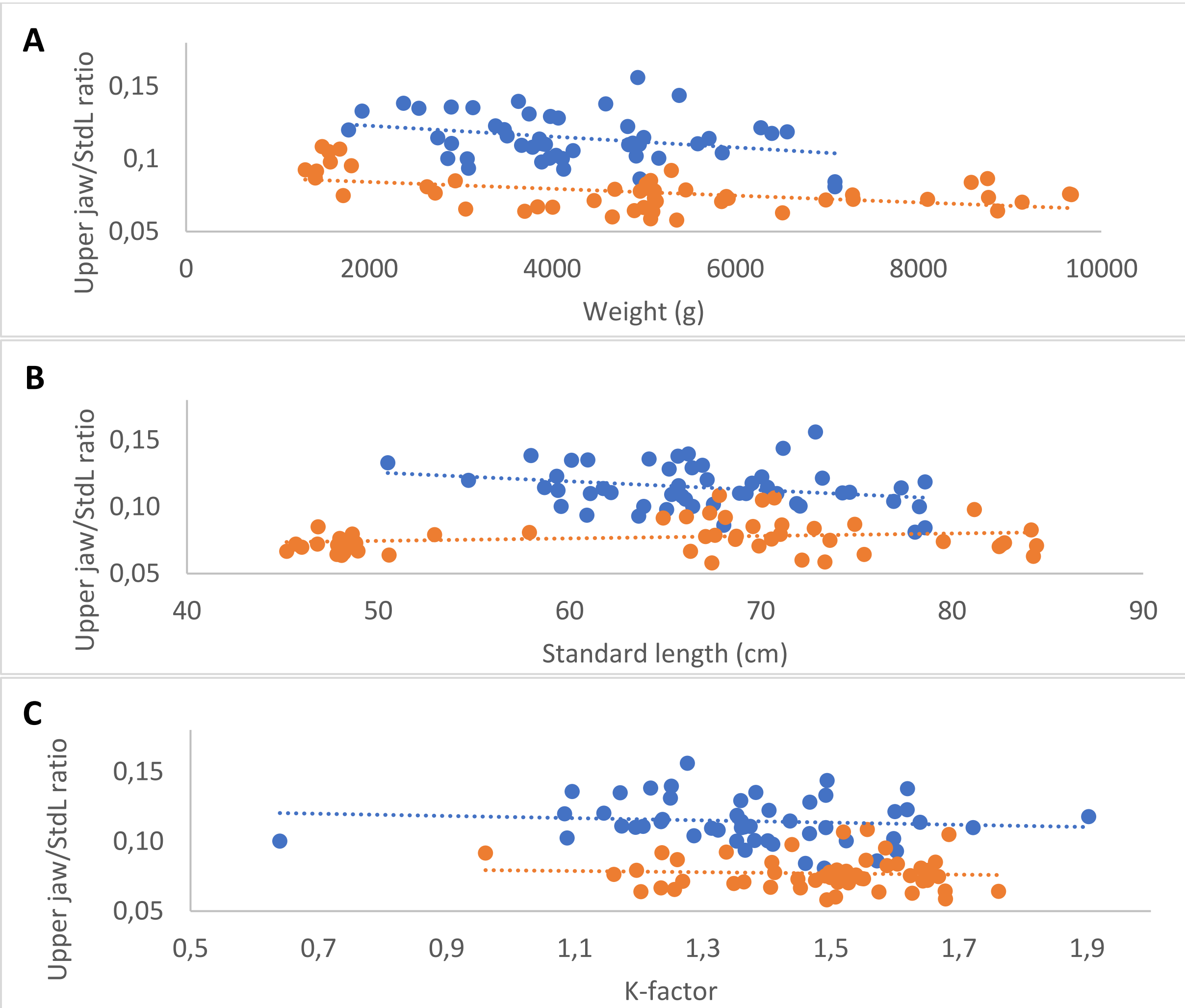

Figure D.2: Morphometrics of the upper jaw for sexually mature (blue) and immature salmon (orange). Upper jaw ratio compared to A: weight, B: standard length and C: K-factor.